Prediction of Harmonic and Intermodulation Performance of Frequency Dependent Nonlinear Circuits and Systems

by

Fahim Shafi

A Thesis Presented to the

FACULTY OF THE COLLEGE OF GRADUATE STUDIES

KING FAHD UNIVERSITY OF PETROLEUM & MINERALS

DHAHRAN, SAUDI ARABIA

In Partial Fulfillment of the
Requirements for the Degree of

MASTER OF SCIENCE

In

ELECTRICAL ENGINEERING

December, 1994

Prediction of Harmonic and Intermodulation Performance of Frequency Dependent Nonlinear Circuits and Systems

BY

Fahim Shafi

A Thesis Presented to the

FACULTY OF THE COLLEGE OF GRADUATE STUDIES

KING FAHD UNIVERSITY OF PETROLEUM & MINERALS

DHAHRAN, SAUDI ARABIA

In Partial Fulfillment of the
Requirements for the Degree of

MASTER OF SCIENCE

In

Electrical Engineering

December 1994

KING FAHD UNIVERSITY OF PETROLEUM AND MINERALS
DHAHRAN, SAUDI ARABIA

This thesis, written by

Fahim Shafi

under the direction of his Thesis Advisor, and approved by his Thesis committee, has been presented to and accepted by the Dean, College of Graduate Studies, in partial fulfillment of the requirements for the degree of

MASTER OF SCIENCE IN ELECTRICAL ENGINEERING

Thesis Committee:

Dr. M. T. Abuelma'atti (Chairman)

Dr. A. R. K. Al-Ali (Member)

Dr. I. M. Naqvi (Member)

Dr. Z. J. Saati (Member)

Dr. J. Zrida (Member)

Dr. A. M. Al-Shehri
Chairman
Electrical Engineering Department

Dr. Ala H. Rabeh
Dean, College of Graduate Studies

Date: 4.1.94

Dedicated to

the memory of my brother

Acknowledgment

I wish to thank my thesis advisor Dr. M.T.Abuelma'atti whose guidance and supervision made this work possible. His support, encouragement and help was infallible during the course of research. His patience, attention and understanding made the experience both enjoyable and rewarding.

I also wish to thank my thesis committee members Dr.Al-Ali, Dr.Naqvi, Dr.Saati and Dr.Zrida for their cooperation and invaluable advice which helped me immensely during my work.

Acknowledgement is due to Electrical Engineering Department, King Fahd University of Petroleum & Minerals, which, under the patronage of Dr. Abdallah M. Al-Shehri, provided financial support in the form of teaching assistantship.

My friends and colleagues for almost a decade, Rizwan Ali Tiwana and Atif Nazir Cheema, deserve a special mention. Their presence was a source of inspiration and consolation during my tenure at the university.

The present and former graduate students of the department, Haroon Khan and Azher Rana remain my mentors in the professional arena.

Special thanks are due to Irfan Ali and Adnan Kiyani whose companionship proved to be a refreshing experience.

Haroon Rafique, presently at Georgia Institute of Technology(USA), was particularly helpful in obtaining research material from abroad. I am also grateful to laboratory technicians Mr.Farazi, Mr.Shams and Mr.Hindawi for their assistance and cooperation.

Contents

List of Tables

List of Figures

Abstract

Name: **Fahim Shafi**

Title: **Prediction of Harmonic and Intermodulation Performance of Frequency Dependent Nonlinear Circuits and Systems**

Major Field: **Electrical Engineering**

Date of Degree: **December, 1994**

In this thesis a new simple mathematical model has been presented for the prediction of harmonic and intermodulation performance of nonlinear circuits and systems. The model is capable of predicting the amplitudes of harmonics and intermodulation products generated by excitation of a nonlinear system by a multi-tone input. Some simple measurements and curve-fitting routines are required to determine the model parameters. The model has been validated for sample frequency-selective networks by experimental methods.

Master of Science Degree

King Fahd University of Petroleum and Minerals

Dhahran, Saudi Arabia

December 1994

خلاصة الرسالة

الاسم : فهيم شفيع

عنوان الرسالة : التنبؤ بالتوافقيات و التضمين التبادلى فى الدوائر والانظمة ذات الخواص غير الخطية المعتمدة على الذبذبة

التخصص : الهندسة الكهربائية

تاريخ الشهادة : ديسمبر ١٩٩٤م

فى هذه الاطروحه تم استنباط نموذج رياضى مبسط يمكن استخدامه فى التنبؤ بالتوافقيات و التضمين التبادلى فى الدوائر والانظمة ذات الخواص غير الخطية المعتمدة على الذبذبة. و يمكن باستخدام النموذج المقترح التنبؤ بسعه التوافقيات و التضمين التبادلى الناتجه من ادخال اشارات متعدده فى اى نظام غير خطى. وللحصول على هذا النموذج تم اجراء عدد من القياسات و استخدام طرق حاسوبيه لاستنباط المنحنيات اللازمه لهذا النموذج. و قد اجري العديد من التجارب على دوائر الكترونيه مختلفه اثبتت صلاحية النموذج المقترح.

درجة الماجستير فى العلوم

جامعة الملك فهد للبترول و المعادن

الظهران – المملكة العربية السعودية

ديسمبر ١٩٩٤م

Chapter 1

Introduction

1.1 Overview

Physical systems, in general, are nonlinear in nature. It may be possible to represent such systems by linear models when perturbed over a restricted operating range, however such processes can be accurately characterized only by nonlinear models.

Communication systems employ numerous circuits and systems that exhibit nonlinearities. These nonidealities result in degradation of the system performance. Active filters and amplifiers form the basic building blocks of modern communication hardware. At low frequencies, active filters and amplifiers are built around discrete BJT, JFET and MOSFET transistors. At relatively high frequencies, such systems are usually composed of operational amplifiers and current-conveyors in addition to external passive elements. At very high frequencies, traveling-wave-tubes (TWT),

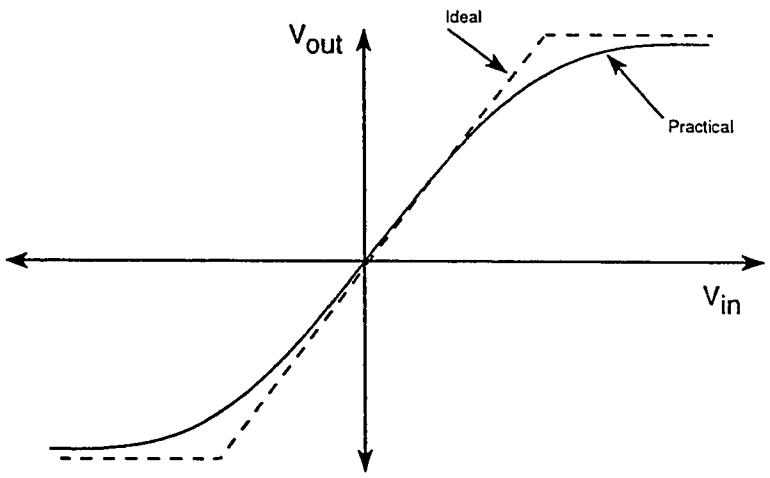

Figure 1.1: Input-Output Characteristics of Operational Amplifier

magnetrons and klystrons are used. TWTs and klystrons are inherently nonlinear, and systems incorporating these devices exhibit distortion in both amplitude (AM-to-AM) and phase (AM-to-PM). Fig. 1.1 shows the input-output characteristics of a typical operational amplifier.

Harmonics of the fundamental frequency are produced at the output when such nonlinear systems are perturbed by a single carrier at the input. In the presence of multiple-carrier input, intermodulation products (Fig. 1.2) are generated in addition to the harmonics [1]. Although the harmonics and intermodulation products are attenuated to a large extent due to the finite bandwidth of communication circuits, selective filter sections operated at large signal levels can exhibit jump resonance [2].

Jump phenomenon is an abrupt change in the output of a feedback circuit with active devices, having nonlinear dynamic characteristics, when the frequency and/or

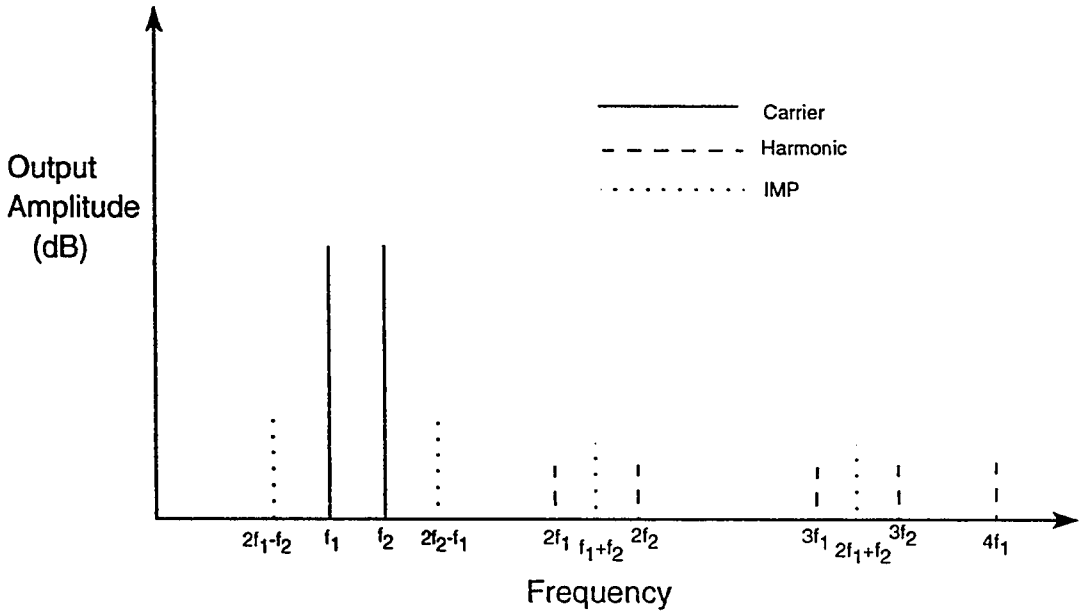

Figure 1.2: Partial Frequency Spectrum of Two-tone Intermodulation

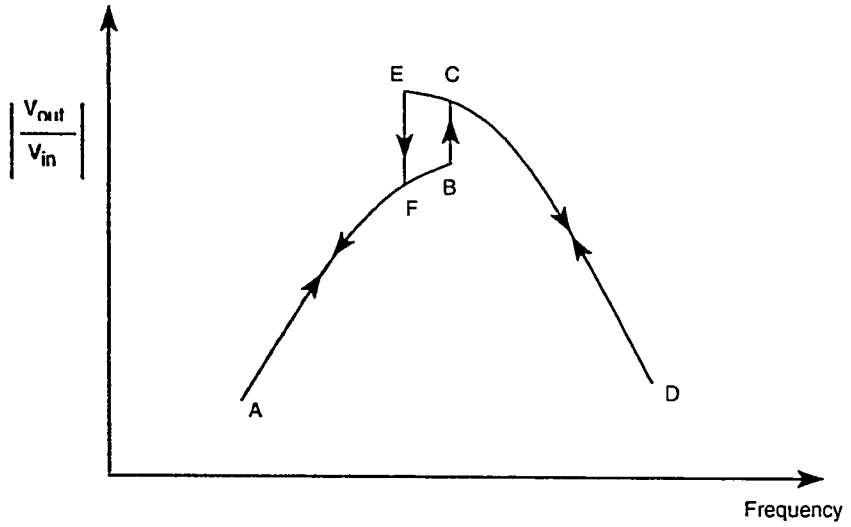

Figure 1.3: Jump Phenomenon in Band-Pass Filter

the amplitude exceeds a certain value (Fig. 1.3). For example, the primary cause of the jump resonance in active-RC filters is the inability of the operational amplifiers to respond, when it is forced to change its output volatge at a rate faster than the slew rate [3].

Prediction of harmonic and intermodulation performance of systems incorporating nonlinear elements such as active filters and amplifiers is, therefore, essential. A prerequisite for such analysis is the mathematical modeling of the performance of these nonlinear elements. It is essential that models for the nonlinearities be as accurate as possible so as to obtain meaningful results by simulation of communication circuits and subsystems.

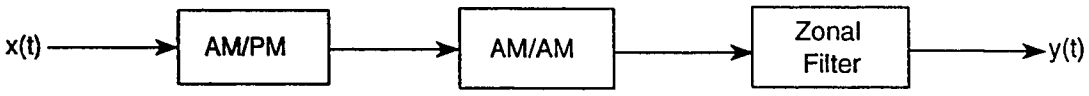

Figure 1.4: Envelope and Phase Format of a Band-Pass Memoryless System

1.2 Literature Review

The nonlinear effects in circuits can be frequency-selective or frequency-independent. The circuits that do not exhibit any significant frequency selectivity can be represented by 'memoryless' models (Fig. 1.4) [4]. These models are based on the instantaneous input-output characteristics and can be characterized by a complex functional relationship given by Equation 1.1.

$$\bar{y}(t) = \bar{G}\,[\bar{x}(t)] \tag{1.1}$$

where $\bar{x}(t)$ and $\bar{y}(t)$ are the complex envelopes of the input and output to the system respectively.

The AM/AM and AM/PM effects, g(.) and f(.) depend only on the modulus of the input envelope and therefore they can be related to the output more accurately by Equation 1.2.

$$\bar{y}(t) = \bar{g}(|\bar{x}(t)|)\, exp\,[j\,[f(|\bar{x}(t)|) + \angle(\bar{x}(t))]] \tag{1.2}$$

Circuits with pronounced frequency-selective effects, for example filters and narrowband amplifiers, can only be represented by models with frequency-dependent

parameters.

Several models have been proposed in literature for the prediction of amplitudes of harmonics and intermodulation products. Some mathematical techniques based on these models have also been suggested.

Volterra series [5] approach is based on a direct relationship to the impulse response of a linear system. A Volterra series is a Taylor series described by the following relation, assuming no constant (dc) response.

$$Y(t) = \sum_{n=1}^{\infty} Y_n(t) \tag{1.3}$$

Each term $Y_n(t)$ in Equation 1.3 is described by an n-fold convolution as:

$$Y_n(t) = \int_{-\infty}^{\infty} \ldots \int_{-\infty}^{\infty} h(T_1, T_2, \ldots, T_n)\, x(t - T_1) \ldots x(t - T_n) dT_1 \ldots dT_n \tag{1.4}$$

where $h(.)$ is the system impulse response and $x(.)$ is the input to the system.

Heathman et al. [6] have characterized the performance of a two-port nonlinear reference network by Volterra series and the results have been compared with the predictions of a quadrature model of the same network.

However, a deficiency in Volterra series models is the justification of truncating the series at some order. The complexity of measurements limits the use of such models to mild nonlinearities with small excitation signals only.

Hetrakul [7] has suggest a nonlinear quadrature model for a TWT type amplifier based on a structure similar to that proposed by Shimbo [8] and later used by Eric [9]. It consists of two envelope nonlinearities parallel to each other, one in the

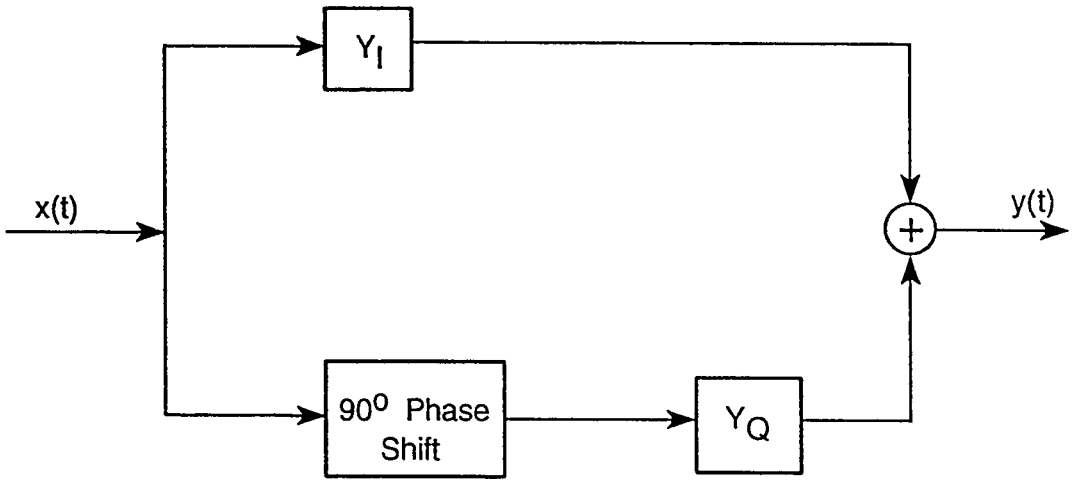

Figure 1.5: Inphase and Quadrature Band-Pass Memoryless System Model

phase and the other in the quadrature path (Fig. 1.5). S_I represents the inphase component whereas S_Q is the quadrature component of the system nonlinearity.

The portion of output wave falling in the same spectral zone as the band-limited input wave is described in terms of the envelope of the input wave, rather than its instantaneous value [10]. Hetrakul [7] has used modified Bessel function of first and second kind to approximate the input-output characteristics of the TWT amplifier.

Poza et al. [11] have extended the memoryless model based on the observation that AM/AM and AM/PM curves measured at different frequencies of the unmodulated sinusoid tend to maintain their shape when plotted on dB~dB scale and phase~dB scale respectively. A serial block structure has been proposed with pure phase and pure amplitude filters at the output.

Saleh [10] has presented two-parameter formulas for AM/AM and AM/PM distortion for the nonlinear quadrature model of a TWT amplifier. A closed form expression has been obtained for the output of a TWT amplifier excited by two phase-modulated carriers. A frequency-dependent quadrature model has also been proposed whose parameters are obtained by single-tone measurements.

Abuelma'atti [12] has also proposed a nonlinear quadrature model for TWT amplifiers exhibiting frequency-dependent amplitude and phase nonlinearity. In-phase and quadrature nonlinearities are expressed in the form of Bessel function and the frequency-dependent coefficients are obtained by using mean-square-error curve-fitting procedure.

Sasaki et al. [13] have proposed a technique for the prediction and measurement of intermodulation performance of systems with weak nonlinearities and multiple carrier input.

Bowron has adopted the harmonic balance evaluation technique extensively [1, 14, 15] for a comparative study of nonlinear distortion effects in active filters and has proposed several circuits with reduced harmonic distortion [2]. He has taken into account the frequency-dependent effects of operational amplifiers by modeling them (Fig. 1.6) as a frequency-independent input nonlinearity (Equation 1.5) followed by a linear frequency-dependence (Equation 1.6).

The influence of finite dynamic range on the frequency response of the system is determined by considering the amplifier as exhibiting a saturation-type nonlinearity.

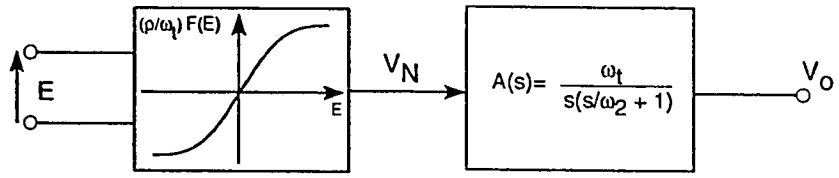

Figure 1.6: Nonlinear Two-pole Model of Differential-Input Operational Amplifier

The linear block represents the small-signal finite-bandwidth performance and the input limiter represents the dominant nonlinearity at high frequencies.

$$V_N = \frac{\rho}{\omega_t} F(E) = \frac{\rho}{\omega_t} \tanh\left[\frac{\omega_t}{\rho} E\right] \tag{1.5}$$

$$A(s) \simeq \frac{\omega_t}{s\left[\frac{s}{\omega_2} + 1\right]} \tag{1.6}$$

where V_N is the output of the nonlinearity, E is the input error signal, ρ is the slew rate, ω_t is the gain-bandwidth product, $A(s)$ is the open-loop gain and ω_2 is the second pole frequency of the amplifer.

A similar device model has been proposed by Abuelma'atti [16] for the input-output nonlinearity and the gain-frequency characteristics of a typical bipolar operational amplifier. A closed form expression has been derived for the output signal of the operational amplifier excited by multi-sinusoidal input signal.

Zeng [17] has represented the circuit variables in frequency-domain complex matrix and the nonlinearities by power series to form an intermodulation prediction technique, the 'intermodulation-balance' method. The technique has been verified for single-amplifier filter with a two-tone input signal.

Volterra functional analysis [18], Fourier series, harmonic linearization and describing fuctions [14, 19] have also been used to model nonlinear behavior of systems.

Arnold [20] has discussed the effects of third order intermodulation products in cable television (CATV) system and presented a curve showing the required level of such products for high quality performance.

Borys [21] has studied the harmonic and intermodulation distortion in single-amplifier filters and presented a relationship between different measures for nonlinear effects in such circuits.

Billam [22] has carried out similar studies on positive feedback active filter networks while Bowron et al. [1] have presented the effect of both linear and nonlinear imperfections of operational amplifiers on the frequency response of a bandpass multiple-negative-feedback active filter.

Forsen et al. [23] have analyzed a model for operational amplifiers in active-RC circuits described by a third order nonlinear differential equation.

Blum [4] has reviewed the state of the art models for nonlinear power amplifiers such as TWTs and analyzed them critically. A new model has been proposed in an attempt to rectify some of the shortcomings of the previous models.

The various approaches and techniques for mathematical modeling as reported in the literature are discussed in detail in Chapter 2.

1.3 Problem Definition

The mathematical description of the nonlinear characteristics must be of the kind which incorporates the major features of the nonlinear behavior of the device while still offering straightforward means for calculating intermodulation product magnitudes, AM/PM conversion effects etc. Having derived the mathematical model it must be possible to derive its parameters from measurements on the practical network.

As described in the previous section, several attempts have been made to propose a model which is valid for general modulated multi-tone inputs with arbitrary amplitudes. All of the existing models suffer from assumptions or lack generalization and effectively no 'high level' model exists for frequency-dependent devices and circuits [4].

Poza et al.'s [11] model assumes constant curve shapes of amplitude and phase characteristics as the frequency is varied. Moreover it gives no clear indication as to the performance of the model for general modulated inputs.

Saleh's model [10] is implicitly constrained by similar limitations as Poza's. The inphase and quadrature curve shapes must remain unaltered as a function of frequency. The proposed frequency-dependent model is complex in terms of structure as well as computation of intemodulation products.

Abuelma'atti [12] has proposed a model that does not suffer from such con-

straints. However, it is computationally more complex and the choice of fitting function has not been discussed properly.

All three models are based on the idea that the response to modulated inputs can be determined, at least approximately, by using a model that is calibrated to produce correct results for single-tone inputs. The assumption may be true for single-tone inputs varying slowly. However this may not be a practical situation. Since the system is not linear, the sinusoids can no longer be assumed to be superimposed [4]. The existing models, therefore, do not address the interactions that occur among the indivuidual sinusoidal components which can be viewed as making up a modulated signal.

A major deficiency shared by all the proposed models is the lack of supporting experimental results to verify the model performance. Experimental data obtained previously has been used as reference in most cases which casts some doubt on the practical accuracy of these models.

It is apparent that a mathematical model is desired which is simple enough for real-time computation applications and is valid for general modulated inputs with arbitrary amplitudes. This thesis work aims at proposing such a model.

The proposed model is expected to be simpler in terms of structure as well as computing functions. Once the model has been derived using experimental data, its performance shall be evaluated practically with inputs of general amplitudes and frequencies. The model shall also be verified for sample circuits of various frequency-

selective networks.

The following steps shall be taken to achieve this objective:

1. Measurement of input-output characteristics of a nonlinear frequency-dependent circuit.

2. Approximation of transfer characteristics to a closed mathematical form.

3. Measurement of harmonic and intermodulation distortion of the circuit.

4. Computation of curve-fitting coefficients for the scaling functions.

5. Experimental verification of the proposed model.

1.4 Thesis Contribution

The thesis presents a new simplified model which attempts to rectify the drawbacks of existing models. The model is supported by computer software for mathematical computation and associated tasks.

Experimental results have been included to establish the validity of the proposed structure. The model was tested for various circuits representing nearly all types of frequency-selective effects in circuits, for example, low-pass, high-pass, band-pass and band-reject filters. The approximating functions were selected to emulate the circuit responses and minimize the effort involved in curve-fitting.

An alternate structure based on the existing idea of single-tone measurements of input-output characteristics was simulated and tested against experimental results. It was found that for multi-tone inputs with arbitrary frequencies and amplitudes, the model is not accurate.

1.5 Thesis Organization

The thesis is organized in the following sequence:

Chapter 1 gives a brief introduction about the effects of nonlinearities on systems with special stress on communication circuits. A concise literature review highlights the attempts and approaches adopted in the area. A brief outline of the thesis work is also presented.

Chapter 2 deals specifically with the existing mathematical models of nonlinear devices, circuits and systems. Drawbacks of these models have also been discussed with special emphasis on the need for a generalized and simplified model.

Chapter 3 describes the proposed model with a brief introduction to the strategy adopted and the alternate modeling approach considered during the course of research. It also addresses the choice of fitting functions for the model blocks. Four curves and their fitting functions are presented to coincide with the circuits tested experimentally.

Experimental results for the circuits tested are presented in Chapter 4. The

predicted amplitudes and observed measurements for four sample circuits have been included for a comparative study.

Chapter 5 concludes the thesis work and some suggestions have been made regarding the directions for future work in this area.

Appendix A includes the software developed in C language to compute the amplitudes of harmonic and intermodulation products generated by the interaction of arbitrary number of signals with desired amplitudes in the nonlinear system. An auxiliary algorithm has been developed to generate a set of input frequencies for which none of the harmonics and intermodulation products overlap each other, given a finite order of nonlinearity. This pre-condition is aimed at minimizing the error due to superimposing effects of harmonics and intermodulation products.

Chapter 2

Modeling of Nonlinear Systems

2.1 Introduction

Communication circuits and systems respond to stimuli in two domains, power and frequency. Nonidealities in such systems, therefore, result in the distortion of both amplitude and phase. Several attempts have been made to develop a mathematical model capable of predicting the performance of devices and circuits with frequency-dependent nonlinearities under varying conditions.

Most analytical studies of communication systems have assumed purely amplitude-limited characersitics. This assumption, though greatly simplifying the analysis, does not include the nonlinear phase effects, which have significant bearing on communication system performance [7].

The chapter summarizes all the significant attempts made in this direction as

reported in the literature. The authors have presented both, frequency-independent and frequency-dependent models in the course of their research. A critical evaluation and a comparative study is presented, following a description of these models, with special emphasis on the need for further work in this area.

Three models have been discussed in the following sections to give the reader an overview of the contemporary approaches towards modeling of nonlinear devices, circuits and systems.

2.2 Poza et al.'s Model

Poza, Sarkozy and Berger [11] presented a computer simulation model capable of predicting the performance of a high data-rate end-to-end communication system for biphase and quadri-phase continuous phase shift keying (CPSK) transmission. The simulation results have been compared with the laboratory measurements to verify the simulation procedure. A parameteric sensitivity analysis is included to evaluate the effect of different signal distortion phenomena on the link performance.

This model appears to be the first attempt at extending the frequency-independent 'memoryless' models based on the observation that the curves for output power and the output phase seem to maintain nearly the same shape when plotted on a dB scale against the input power. Thus both AM/AM and AM/PM curves for different frequencies can be obtained by applying appropriate horizontal and vertical shifts

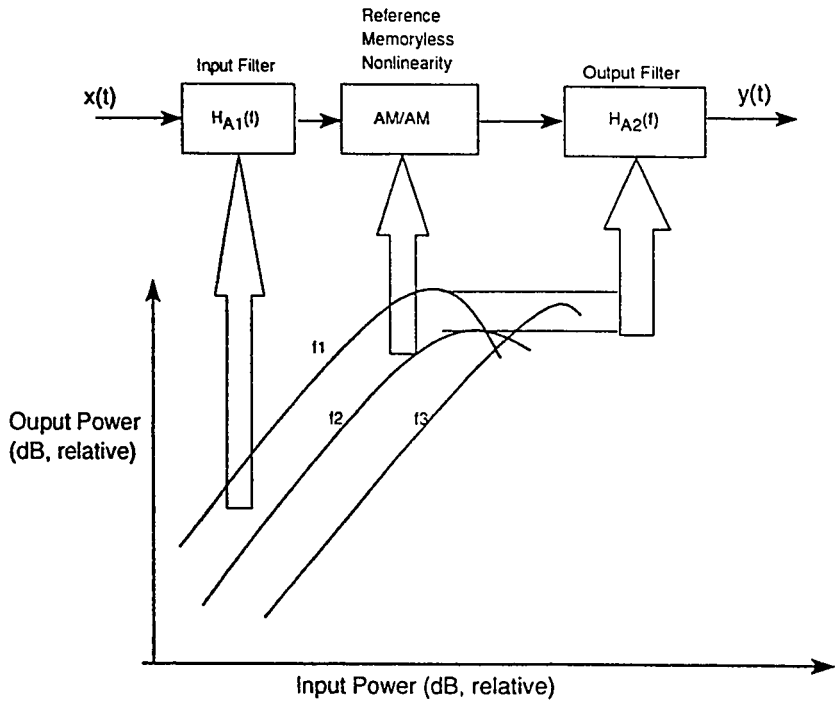

Figure 2.1: Construction of Frequency-Dependent AM/AM Block Model

to the reference curve of these characteristics measured at a single frequency.

In the case of AM/AM distortion (Fig. 2.1) the shifts on a dB scale are equivalent to multiplication by scaling factors on real scale (abscissa and ordinate). This scaling can be implemented by amplitude-only filters preceeding and following the reference AM/AM nonlinearity.

$H_{A1}(f)$ and $H_{A2}(f)$ are pure amplitude filters included to incorporate horizontal and vertical shifts whereas the AM/AM block represents the reference nonlinearity measured at a single frequency.

The AM/PM curves (Fig. 2.2) for were also experimentally observed to maintain

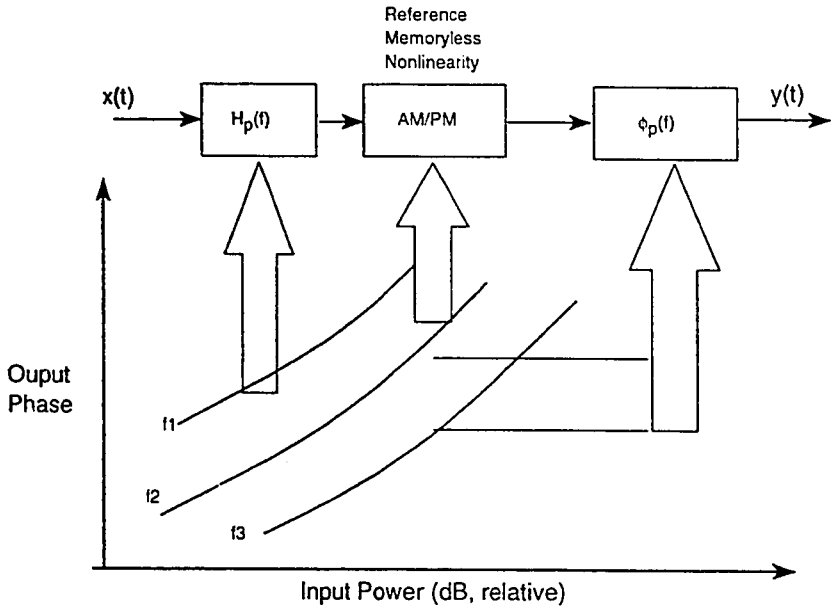

Figure 2.2: Construction of Frequency-Dependent AM/PM Block Model

shapes for different frequencies. The horizontal shifts can be implemented similarly by amplitude-only filters. The vertical shifts on phase versus output power(dB) are realized by phase-only filters.

$H_p(f)$ is the pure amplitude filter and $o_p(f)$ is the pure phase filter to account for the horizontal and vertical shifts of the phase versus output power curve respectively.

The resulting model proposed by Poza et al. [11] has a serial block structure (Fig. 2.3) with an array of pure amplitude and pure phase filters. Some filters have been combined for convenience.

The simulation and measured results are reported to be accurate upto 0.25dB to 0.4dB.

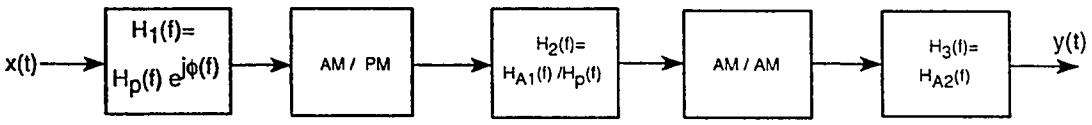

Figure 2.3: Poza et al.'s Serial Block Structure for Frequency-Dependent TWT Amplifier

2.2.1 Drawbacks

The basic assupmtion in Poza et al.'s model, that AM/AM and AM/PM curves maintain shapes at different frequencies, may not be always valid. The authors have attempted to compensate this through an elaborate curve-fitting procedure to find a curve which best fits all the measured values [4]and determine the best shift values for each frequency. The procedure involved is quite complicated and it may be adequate to fit the curve at a nominal frequency and determine the best shifts instead.

The model should give good results for single-tone unmodulated inputs by virtue of its construction but its accuracy for such unmodulated tones relies only on the validity of the constant shape of the AM/AM and AM/PM curves. The performance of the model for general modulated inputs is unclear [4].

2.3 Saleh's Model

Saleh [10] proposed frequency-independent and frequency-dependent nonlinear models of traveling-wave tube (TWT) amplifiers. He has used the two popular structures for the frequency-independent model, that are, the amplitude-phase and the inphase-quadrature block formats. Saleh has derived two-parameter formulas for both the models. The parameters for these models were obtained by single-tone input-output measurements and computation procedures.

2.3.1 Frequency-Independent Amplitude-Phase Model

For the input signal $x(t)$ given by Equation 2.1

$$x(t) = r(t)\cos[\omega_o t + v(t)] \tag{2.1}$$

the output $y(t)$ of the amplitude-phase model is

$$y(t) = A[r(t)]\cos[\omega_o t + v(t) + \Phi[r(t)]] \tag{2.2}$$

where ω_o is the carrier frequency, $r(t)$ and $v(t)$ are the modulated envelope and phase respectively and $A(r)$ and $\Phi(r)$ are odd and even functions of r respectively.

Saleh proposed the following two-parameter formulas for the amplitude and phase functions:

$$A(r) = \frac{\alpha_a r}{1 + \beta_a r^2} \tag{2.3}$$

$$\Phi(r) = \frac{\alpha_o r^2}{1 + \beta_o r^2} \tag{2.4}$$

2.3.2 Frequency-Independent Inphase-Quadrature Model

Saleh has obtained similar parametric equation for inphase-quadrature model. The parallel structure [7, 9] was used for this purpose. If the input is given by Equation 2.1, the output is the sum of inphase and quadrature components (Fig. 2.4).

$$y(t) = p(t) + q(t) \tag{2.5}$$

where

$$p(t) = P[r(t)]\cos[\omega_o t + \psi(t)] \tag{2.6}$$

and

$$q(t) = -Q[r(t)]\sin[\omega_o t + \psi(t)] \tag{2.7}$$

which is equivalent to stating that

$$P[r(t)] = A[r(t)]\cos[\Phi[r(t)]] \tag{2.8}$$

and

$$Q[r(t)] = A[r(t)]\sin[\Phi[r(t)]] \tag{2.9}$$

Eric [9] proposed representing $P(r)$ and $Q(r)$ by odd polynomial of r which requires a large number of coefficients to fit realistic TWT amplifier data [10]. Hetrakul [7] used two-parameter formulas involving modified Bessel function of the first

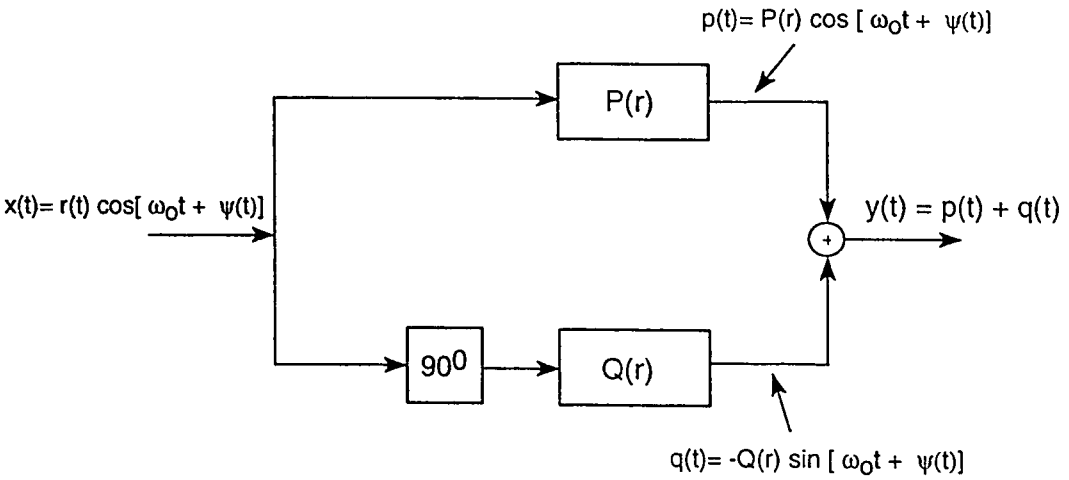

Figure 2.4: Quadrature Nonlinear Model for Power Amplifier

kind. Saleh has proposed the represent $P(r)$ and $Q(r)$ by two-parameter formulas of the form:

$$P(r) = \frac{\alpha_p r}{1 + \beta_p r^2} \tag{2.10}$$

and

$$Q(r) = \frac{\alpha_q r^3}{(1 + \beta_q r^2)^2} \tag{2.11}$$

Saleh has demonstrated the validity of this model by comparing the predicted values with those reported in the literature [24, 25]. A minimum mean-square-error procedure for fitting the formulas to the experimental data has also been discussed.

The application of the proposed model for intermodulation analysis has been described for the case of two-carrier signal and shown to yield a close form expression for the output signal. Similar analysis for multiple-phase modulated carriers has also

been suggested.

2.3.3 Frequency-Dependent Quadrature Model

Saleh has suggested that a frequency-dependent model for TWT amplifiers could be obtained from single-tone measurements of the device. The frequency-dependent inphase and quadrature components of the model can be described as

$$P(r,f) = A(r,f)\cos[\Phi(r,f) - \Phi_o(f)] \tag{2.12}$$

$$Q(r,f) = A(r,f)\sin[\Phi(r,f) - \Phi_o(f)] \tag{2.13}$$

where

$$\Phi_o(f) = \lim_{r \to 0} \Phi(r,f) \tag{2.14}$$

For a given frequency f, equations 2.10 and 2.11 can be made to fit the experimental data for the frequency-dependent case, using the curve-fitting procedure described. The frequency-dependent parameters $\alpha_p(f)$, $\beta_p(f)$, $\alpha_q(f)$, $\beta_q(f)$ could thus be obtained (Fig. 2.5).

The filter blocks could be computed to be as follows:

$$H_p(f) = \sqrt{\beta_p(f)}$$

$$G_p(f) = \frac{\alpha_p(f)}{\sqrt{\beta_p(f)}}$$

$$H_q(f) = \sqrt{\beta_q(f)}$$

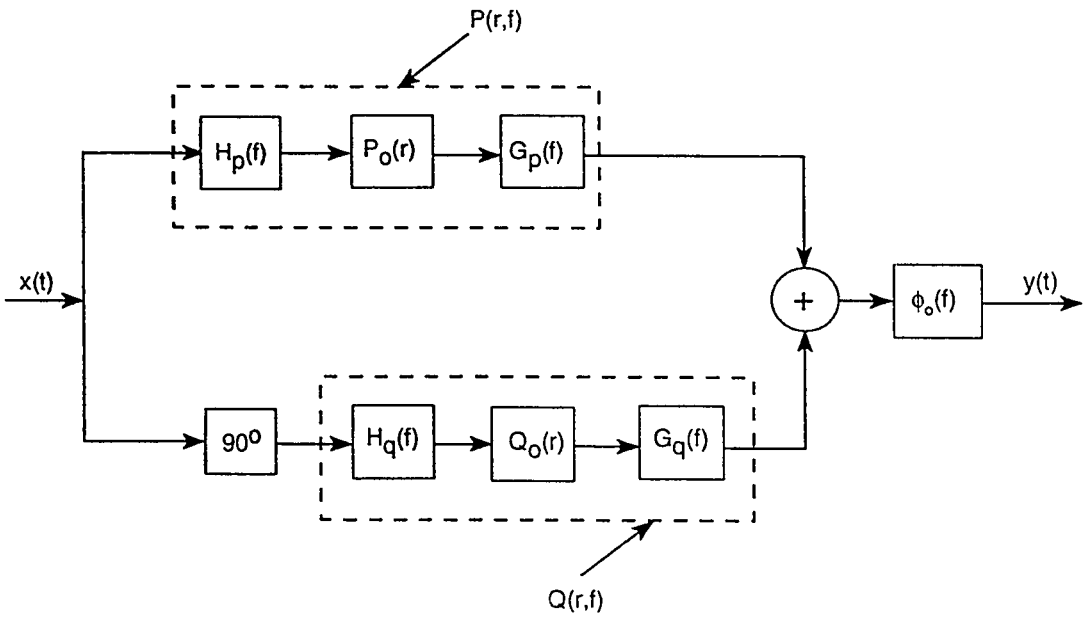

Figure 2.5: Saleh's Frequency-Dependent Quadrature Model of TWT Amplifier

$$G_q(f) = \frac{\alpha_q(f)}{\beta_q^{3/2}}$$

The normalized frequency-independent envelope nonlinearities can be defined as:

$$P_o(r) = \frac{r}{1+r^2}$$

$$Q_o(r) = \frac{r^3}{(1+r^2)^2}$$

Saleh's model, therefore, is essentially based on the classical structure of inphase and quadrature nonlinearities with the component blocks adjusted to suit the experimetal data. The generalized equation proposed for this purpose is given by:

$$z(r) = \frac{\alpha r^n}{(1+\beta r^2)^\nu}$$

where $n = 1, 2, 3$ and $\nu = 1$ or 2

The operations performed on the single-tone input in the inphase branch can summarized as follows: the input amplitude is scaled by $H_p(f)$ and the resulting signal passes through the frequency-independent nonlineairty $P_o(r)$ and finally the output amplitude is scaled by filter $G_p(f)$. Similar steps of operation are undertaken on the quadrature path. The filter operations in each branch can be interpreted as subjecting the signal to a linear filter with real frequency response.

The terminal block at the output represents a linear, all-pass network having an amplitude reponse of unity and a phase response of $\Phi_o(f)$.

2.3.4 Drawbacks

Saleh's model is valid only for single-tone input signals by virtue of the procedure used to contruct it [10, 12]. Its validity for arbitrary input signal is a conjecture that remains to be confirmed experimentally.

The proposed model is dual to that of Poza's to some extent. Poza's model is contrained to keep the AM/AM and AM/PM curves of constant shape whereas Saleh's model is implicitly constrained to keep the inphase and quadrature curve shapes identical as a function of frequency [4]. The fact that Saleh has used frequency-dependent coefficients does not alter this assumptions since the functional forms he has picked are very special and they allow these coefficients to be factored out.

It can be shown that constraining the inphase and quadrature curves to maintain shape is essentially different from applying similar requirement to amplitude and phase curves. This implies that even for single-tone input signal, Poza's and Saleh's models must be different. The two models will yield identical results for AM/AM and AM/PM characterisitics only if abscissas are scaled identically as a function of frequency [4].

Since both models are based on single-tone measurements and they differ even in the interpretation of these measurements, therefore their performance for general modulated inputs requires further investigation.

2.4 Abuelma'atti's Model

Abuelma'atti [12] has proposed frequency-independent and frequency-dependent nonlinear quadrature models for TWT amplifiiers exhibiting both AM/AM as well as AM/PM conversion. The models have a similar premise as Saleh's. It is claimed that the frequency-dependent quadrature model is valid for multi-tone input signals with arbitrary amplitudes by virtue of the procedure used to construct it.

2.4.1 Frequency-Independent Quadrature Model

If the input signal to the quadrature model is given as:

$$x(t) = A\cos(2\pi f_o t + \theta_o) \tag{2.15}$$

then the output is given by the sum of inphase and quadrature components

$$Y_I(t) = F(A)\cos[\psi(A)]\cos(2\pi f_o t + \theta_o) \tag{2.16}$$

$$Y_Q(t) = F(A)\sin[\psi(A)]\sin(2\pi f_o t + \theta_o) \tag{2.17}$$

where $F(A)\cos[\psi(A)]$ and $F(A)\sin[\psi(A)]$ are the inphase and quadrarture nonlinearies deduced from the measureable frequency-independent amplitude nonlinearity $F(A)$ and AM/PM conversion $\psi(A)$ of the amplifier.

The two nonlinearities can be represented in the form of Bessel function as follows:

$$F(A)\cos[\psi(A)] = \sum_{n=1}^{N} \gamma_{nI} J_1\left(\frac{n\pi A}{D}\right) \tag{2.18}$$

$$F(A)\sin[\psi(A)] = \sum_{n=1}^{N} \gamma_{nQ} J_1\left(\frac{n\pi A}{D}\right) \tag{2.19}$$

where $J_1(.)$ is the Bessel function of first kind of order one, $2D$ is the dynamic range of the input voltage (in Volts) and $\gamma_{nI(Q)}$ can be obtained by using minimum mean-square-error curve-fitting procedure to fit equations 2.18 and 2.19 to the experimental data.

Using equations 2.18 and 2.19, the amplitude $V_{(a_1,a_2,\ldots,a_M)}$ of an output product of frequency

$$\sum_{m=1}^{M} a_m f_m \tag{2.20}$$

resulting from exciting the amplifier by a multi-tone input of the form

$$\sum_{m=1}^{M} V_m \cos 2\pi f_m t \tag{2.21}$$

is given by [26] :

$$V_{(a_1,a_2,\ldots,a_M)} = \left[\left(V_{(a_1,a_2,\ldots,a_M)I}\right)^2 + \left(V_{(a_1,a_2,\ldots,a_M)Q}\right)^2\right]^{1/2} \tag{2.22}$$

where

$$V_{(a_1,a_2,\ldots,a_M)I(Q)} = \sum_{n=1}^{N} \gamma_{nI(Q)} \prod_{i=1}^{M} J_{|a_i|}\left(\frac{n\pi V_i}{D}\right) \tag{2.23}$$

and a_m is a postive or negative integer or zero, $J_{|a_i|}$ is the Bessel function of first kind of order $|a_i|$. and $\sum_{m=1}^{M}|a_m|$ is the order of output product and is an odd integer.

2.4.2 Frequency-Dependent Quadrature Model

Abuelma'atti's frequency-dependent model is based on the idea that a quadrature model can be derived for each input frequency by minimum mean-square-error curve fitting the data to a generalized formula (Fig. 2.6). This would yield the required frequency-dependent parameters.

The frequency-dependent parameters γ_{nI}, γ_{nQ}, $n \rightarrow N$ can be approximated closely by

$$\gamma_{nI(Q)}(f) = \gamma_{0n_{I(Q)}} G_{n_{I(Q)}}(f) \qquad n = 1 \rightarrow N \tag{2.24}$$

Using Equation 2.23 the model can be modified to include the frequency-dependent effects of Equation 2.24.

Each branch consists of a frequency-independent envelope nonlinearity

$$\gamma_{0nI(Q)} J_1\left(\frac{n\pi A}{D}\right)$$

followed by a scaling filter $G_{nI(Q)}(f)$. The amplitude of the output product of frequency (Equation 2.20) is given by

$$\gamma_{0nI(Q)} \prod_{i=1}^{M} J_{|\alpha_i|}\left(\frac{n\pi V_i}{D}\right)$$

which will be scaled due to the filter by

$$G_{nI(Q)}\left(\sum_{m=1}^{M} \alpha_m f_m\right)$$

The amplitude of the output product of frequency (Equation 2.20) would there-

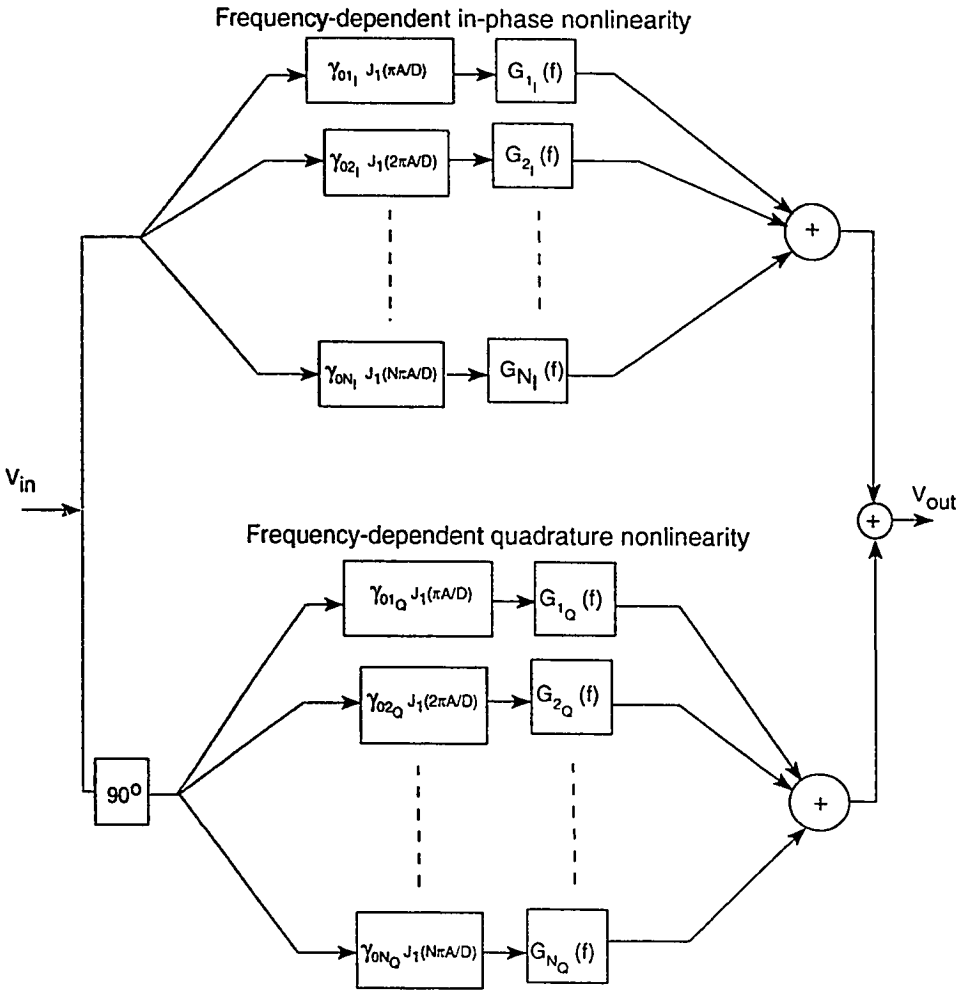

Figure 2.6: Abuelma'atti's Frequency-Dependent Model for TWT Amplifier

fore be given by

$$V_{(a_1,a_2,\ldots,a_M)} = \left[\left(V_{(a_1,a_2,\ldots,a_M)I}\right)^2 + \left(V_{(a_1,a_2,\ldots,a_M)Q}\right)^2\right]^{1/2} \tag{2.25}$$

where

$$V_{(a_1,a_2,\ldots,a_M)I(Q)} = \sum_{n=1}^{N}\left[\left(\gamma_{on_{I(Q)}}\prod_{i=1}^{M} J_{|a_i|}\left(\frac{n\pi V_i}{D}\right)\right) G_{n_{I(Q)}}\left(\sum_{m=1}^{M} a_m f_m\right)\right] \tag{2.26}$$

The frequency-independent (Equation 2.23) and frequency-dependent (Equation 2.26) models are therefore similar, with the coefficients being a function of frequency in the latter.

2.4.3 Drawbacks

Abuelma'atti's model has the advantage of not assuming any curve shapes to remain constant as a function of frequency. However, the model is quite complicated in terms of functions that need to be computed. The accuracy of the model itself is dependent on the number of terms N in equations 2.18 and 2.19.

The curve-shapes are not restrained and could change depending upon the device response and the coefficients. For single-tone inputs, Abuelma'atti's model overcomes the defficiencies of the models discussed previously.

It is, however, possible that the model could be represented in a more efficient way, perhaps by using orthogonal polynomials instead of Bessel functions. This would facilitate the calculation of the coefficients and make it useful for computer simulation.

The paper has not addressed the choice of fitting functions in detail. An example for frequency-dependent coefficient approximation is given as

$$\gamma_n = \gamma_{0n} e^{-\beta_n (f-f_o)^2}$$

where β_n is a constant to be found by curve-fitting, γ_{0n} is the maximum value of γ_n and f_o is the frequency at which γ_n is maximum. This choice of fitting function, however, may not be valid in all cases.

2.5 Conclusions

State of the art models have been presented in this chapter. A comparative study of their advantages and disadvantages has been included.

It is concluded that each model is based on certain assumptions and its validity holds within the confines dictated by them. None of the models was tested experimentally to evaluate the performance in real life situation. The models were essentially compared with the data already available from various sources. The accuracy of results is therefore, liable to be affected by experimental considerations.

All the models were infact derived from the practical characteristics available for the device. The application of these models to determine the harmonic or intermodulation performance has not been discussed in detail in the literature.

The mathematical technique involved in the modeling of these devices and circuits relies on elaborate curve-fitting procedures which renders them less useful for

real-time applications. Moreover, the fitting functions themselves contribute to the complexity of the model and hence the computation overhead.

The need for further analysis of the current models for nonlinear systems with memory is evident [4].

Chapter 3

A New Model for Frequency-Dependent Nonlinear Systems

3.1 Introduction

In most applications, the effects of nonidealities are undesireable. It is therefore necessary that such undesireable effects be predicted for a given system to facilitate the formulation of counter measures. Communication system simulation is aimed at accurate prediction of amplitudes of harmonic and intermodulation products from excitation of nonlinear systems by multi-sinusoidal input.

It is usual to utilize an approximate model of the nonlinear network, chosen to

offer the most direct basis for computation of the intermodulation spectra compatible with acceptably accurate modeling of measured network characteristics.

The techniques and approaches towards mathematical modeling of nonlinear circuits and systems have been discussed in the previous chapter. In conclusion, the need for a simplified mathematical model capable of determining the system response to arbitrary inputs with acceptable degree of accuracy was made apparent.

It has been pointed out earlier that accurate and simplified models exist for frequency-independent circuits and systems. The proposed model shall be expected to account for the frequency-dependent effects in nonlinear systems.

This chapter proposes a new model possessing such attributes and explains the premise of its derivation. The resulting structure is not only simplified but also represents the system with sufficient degree of accuracy. The validity of proposed model is verfied subsequently by predicting the system performance and comparing it with the experimental results.

Active filters are an important class of frequency-dependent circuits used in communication systems. In fact most finite bandwidth amplifiers can also be viewed as wideband filters. Active filters shall, therefore, be used as sample frequency-selective networks to derive and verify the model.

3.2 Evolution of Modeling Approach

The input and output spectra of a nonlinear system are not identical in terms of their frequency components. A multi-tone input to a nonlinear system generates a large number of frequency 'by-products' in the form of harmonics and the intermodulation products.

The output characteristes of a frequency-dependent circuit are therefore expected to depend not only on the input frequency and amplitude but also on the output frequency. This implicitly dictates the need for a frequency-dependent section, both at the input and the output of the model. Poza et al. [11], Saleh [10] and Abuelma'atti [12] have included such filter blocks in their models. However, the mathematical functions describing these blocks are either unclear or they have been derived by tedious curve-fitting of experimental data.

In order to simplify, a modeling approach based on the approximation of input-output charactersitics by power series was adopted. The characteristics were measured at several frequencies and then each coefficient of the power series approximation was plotted against the frequency of measurement. A closed form mathematical expression was obtained by curve-fitting of the data set for the coeffcient versus frequency.

The resultant mathematical expression for the system transfer characteristics

was of the form:

$$V_{out} = \sum_{i=1}^{\infty} k_i(f)\, V_{in}^i \tag{3.1}$$

where each curve-fitting coefficient k_i of the power series approximation is expressed as a function of frequency f.

For single-tone inputs, the model is expected to be very accurate by virtue of the procedure involved in its derivation. The error will be introduced only by the curve-fitting procedures involved. However, the question of applicability of the model to multi-tone input would lead to abstract assumptions.

For example, in the presence of two or more frequencies, the argument f can no longer be assumed to be the frequency of any of the input signals. If f is assumed to be the frequency of the output component for which the amplitude is being calculated, then there is a conflict of cause-and-effect. The nonlinear characteristics of the system would then have to be calculated by an output that has already been generated by this nonlinearity.

The model was simulated by computer software and the results were compared with those obtained experimentally. A large discrepancy was observed between them for the case of multi-tone input.

The approach, however, led to the technique on which the actual proposed model has been based. The derivation procedure for the proposed model is described in the next section.

3.3 Derivation of Proposed Model Structure

It is apparent that any attempt to express the nonlinear behavior of a system as a generalized mathematical function would be restricted to single-tone measurements. For multi-tone inputs, the approach is bound to produce erroneous results.

Heathman et al. [6] have demostrated by using experimental measurements that substantial disparities exist between the prediction of the quadrature model for the intermodulation analysis, using this approach. The conclusion indicates that in order to obtain a more accurate model, measurement of intermodulation product levels, in addition to the envelope and phase characteristics, is necessary.

The strategy evolved for the derivation of the proposed model is, therefore, based on actual measurements of the intermodulation amplitudes, in addition to the AM/AM characteristics. The model parameters have subsequently been derived using these measurements.

The need to simplify the existing models dictates the isolation of the frequency-independent and frequency-dependent nonlinear phenomena of the system in a manner so as to allow separate computation of the two effects. Some adjustments would be needed, both at the input and at the output, to take into account the frequency-dependent effects of the system (Fig. 3.1).

The proposed simplified mathematical model is shown in Fig. 3.2. The model consists of a 'prefilter' $H(j\omega)$, followed by a reference nonlinearity and terminated

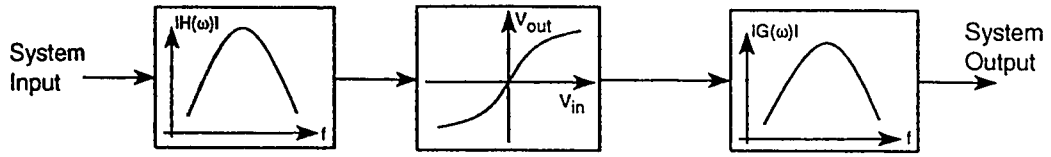

Figure 3.1: Isolated Frequency- Independent and Dependent Behavior

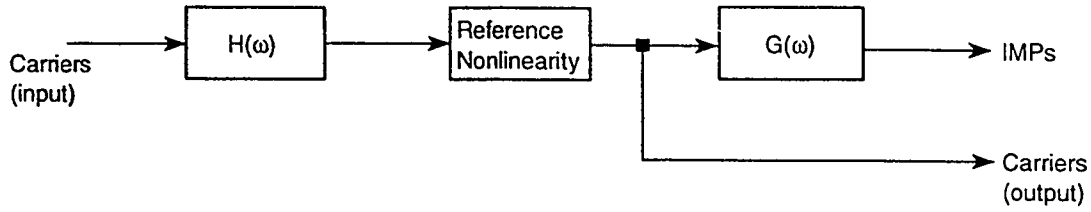

Figure 3.2: Proposed Model for Frequency-Dependent Nonlinear Systems

by the 'postfilter' $G(j\omega)$ to scale the intermodulation products.

The prefilter $H(j\omega)$ has been chosen to be the filter transfer function itself with the passband gain normalized to unity. This enables relative scaling of input carrier signals and hence making the effect of individual sinusoid on the system nonlinearity, a function of its frequency. Mathematically,

$$|H(j\omega)| = \frac{|T(j\omega)|}{|T(j\omega)|_{max}}$$

where $|T(j\omega)|_{max}$ is the magnitude of filter transfer function, measured ideally at a nominal frequency of $\omega = 0$ for low-pass filter, $\omega = \infty$ for high-pass filter, $\omega = \omega_o$ for bandpass filter and $\omega = 0, \infty$ for band-reject filter.

The reference nonlinearity is the power series approximation of input-output characteristics of the filter measured at the respective frequencies mentioned above.

Bonello [27] has suggested a similar method of measurement of harmonic distortion in positive and negative feedback filters by computing the 'distortion factor' in such circuits.

The premise of such measurements is to fix the nonlinearity to a value measured at a certain frequncy and use it as a reference to compute the nonlinear characteristics at other frequencies. This enables the separation of frequency-selective and frequency-independent behavior of the system.

The postfilter section $G(j\omega)$ is derived from the experimental data using curve-fitting functions of the respective filters as described later. The experimental data is compared with that at the output of the reference nonlinearity to determine the scaling factor required for accurate prediction at each frequency. The set of these scaling factors is then plotted against frequency and a closed form mathematical expression is obtained.

The carrier amplitudes need not be subjected to the postfilter since they are already scaled in terms of magnitude by the prefilter and reference nonlinearity blocks.

A similar procedure could be carried out to derive the blocks for prediction of phases of the intermodulation products. The measurement of product phase, howevever, involves almost insurmountable difficulties [6].

As pointed out earlier, the primary motivation behind proposing such a model is to simplify the derivation procedure of opeartional blocks. The following section de-

scribes mathematical functions of the various blocks and the curve-fitting procedure adopted to approximate them.

3.4 Selection of Curve-fitting Functions

3.4.1 Input-Output Characteristics

The typical input-output charactersitics of an operational amplifer were shown in Fig. 1.1. Several mathematical functions can be used to approximate these characteristics. The aim of the procedure, however, remains the same: an accurate representation of the set of data with minimum number of curve-fitting coefficients. Another consideration to this effect would be the ease in computation of amplitudes on harmonics and intermodulation products based on this approximation.

Some fitting functions that can be used for this purpose are:

$$y = a(1 - e^{-x/b}) \tag{3.2}$$

$$y = a\tanh(bx) \tag{3.3}$$

$$y = \sum_{n=0}^{\infty} a_n x^n \tag{3.4}$$

$$y = \sum_{n=0}^{\infty} a_n \cos(nx) + b_n \sin(nx) \tag{3.5}$$

where a and b are the coefficients to be found by curve-fitting experimental data.

The functions may easily be recognized as duals in terms of series expansions but are presented here for brevity. For example, the hyperbolic tangent function (Equa-

tion 3.3) could be represented in terms of an exponential function (Equation 3.2) which in turn is expandable in a power series (Equation 3.4).

The fitting coefficients of equations(3.2) - (3.5) can be obtained using curve-fitting subroutines available on most mainframe computer systems. On the other hand, Abuelma'atti [28] has presented an algorithm based on the Fourier series (Equation 3.5) which can be used to fit measured data to a Fourier model of any order without recourse to discrete Fourier transform or curve-fitting routines.

All of the above fitting functions were implemented and it was found that the power series expansion (Equation 3.4) is the best compromise in terms of computation effort, accuracy and the ease in predicting the amplitudes of frequency components at the output.

A nonlinear device with input x and output y can be described by the power series

$$y = \sum_{n=0}^{\infty} a_n x^n \tag{3.6}$$

The input is given by the summation of sinusoids $x = x_1 + x_2 + x_3 + \cdots + x_M$ where

$$x_i = E_i \cos\theta_i$$

and $\theta_i = \omega_i t + \phi_i$. Equation 3.6 can therefore be written as:

$$y = \sum_{n=0}^{\infty} a_n \left(\sum_{m=1}^{M} x_m \right)^n \tag{3.7}$$

The output y is composed of the sum of all the distinct terms of the form $V\cos\theta$.

where

$$\theta = n_1\theta_1 + n_2\theta_2 + \cdots + n_M\theta_M$$

and the coefficients $n_1, \cdots, n_M$ can take any integer values. V is the amplitude of the harmonic or the intermodulation product. The 'order' of intermodulation product is given by

$$N = |n_1| + |n_2| + \cdots + |n_M| \tag{3.8}$$

Intermodulation or harmonics of order N can be produced only by a system whose characteristics have been approximated by a power series of order equal to or greater than N. A unity order ($N = 1$) frequency component at the output represents the carrier itself.

Sea [29, 30] has presented an algorithm to compute the amplitude of any harmonic or intermodulation product produced by a device described by a power series and having an input consisting of sum of an arbitrary number of sinusoids. The computer software implementation of this algorithm is described in Appendix A.

The frequency-independent reference characteristics in the proposed model for the system are measured at the frequency at which the system transfer function magnitude is maximum ($|T(j\omega)|_{max}$). The system, at this frequency, would be exhibiting the most nonlinear behavior.

Thus, the input-output characteristics of the system are measured at a nominal frequency, say ω_{nom} where the magnitude of its transfer function $|T(j\omega)|$ is maximum. The characteristics are then approximated to a power series using standard

curve-fitting procedures.

3.4.2 Prefilter and Postfilter Blocks

The prefilter $H(j\omega)$ and postfilter $G(j\omega)$ are real (pure amplitude) filters at the input and output. The possible functions to fit the experimental data could be of the following forms:

$$y = a - e^{-\beta(x-x_o)^2}$$

$$y = \frac{\sum_{i=0}^{N} a_i x^i}{\sum_{j=0}^{M} a_j x^j}$$

$$y = \sum_{n=0}^{\infty} a_n \cos(nx) + b_n \sin(nx)$$

A natural choice for curve-fitting such a frequency response, however, would be the magnitude of a generalized filter function.

The most general form of the transfer function of a second order filter section is expressed by [31] Equation 3.9.

$$T(s) = \frac{a_n s^2 + b_n s + c_n}{a_d s^2 + b_d s + c_d} \tag{3.9}$$

The magnitude of the generalized filter transfer function at $s = j\omega$ is given by

$$|T(j\omega)|^2 = \frac{(c_n - a_n\omega^2)^2 + (b_n\omega)^2}{(c_d - a_d\omega^2)^2 + (b_d\omega)^2} \tag{3.10}$$

or

$$|T(j\omega)| = \frac{\sqrt{(c_n - a_n\omega^2)^2 + (b_n\omega)^2}}{\sqrt{(c_d - a_d\omega^2)^2 + (b_d\omega)^2}} \tag{3.11}$$

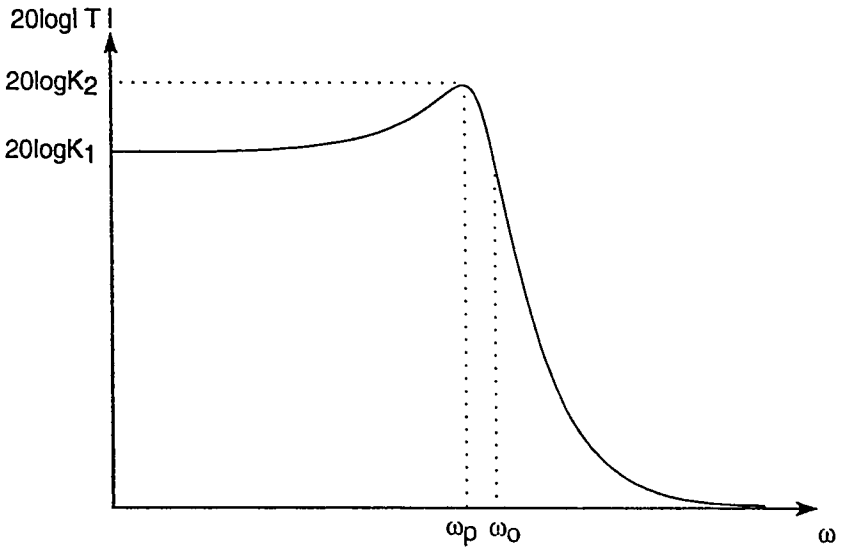

Figure 3.3: Generalized Low-Pass Filter Response

By proper selection of the coefficients, Equation 3.11 can be used to fit the data for the magnitude response of any type of filter, as explained in the subsequent sections.

Low-Pass Filter

A typical second order active low-pass filter has a frequency response as shown in Fig. 3.3. The corresponding transfer function for the filter is given by

$$T(s) = \frac{c_n}{a_d s^2 + b_d s + c_d} \tag{3.12}$$

and the resulting expression for magnitude is given by

$$|T(j\omega)| = \frac{c_n}{\sqrt{(c_d - a_d\omega^2)^2 + (b_d\omega)^2}} \tag{3.13}$$

The curve-fitting parameters c_n, a_d, b_d, c_d can be derived directly by visual inspection of the frequency response as follows:

$$c_n = K_1\omega_p^2 \tag{3.14}$$

$$a_d = 1 \tag{3.15}$$

$$b_d = \frac{\omega_p}{Q} \tag{3.16}$$

$$c_d = \omega_p^2 \tag{3.17}$$

where [32]

$$Q = \frac{K_2}{K_1} \tag{3.18}$$

and

$$\omega_p = \omega_o\sqrt{1 - \frac{1}{2Q^2}} \tag{3.19}$$

and ω_o is the half-power or cut-off frequency of the filter at which

$$|T(j\omega_o)| = \frac{|T(j\omega)|_{max}}{\sqrt{2}}$$

K_1 is the dc gain ($|T(j0)| = K_1$), whereas K_2 is the gain of the filter at $\omega = \omega_p$ for a low-pass filter.

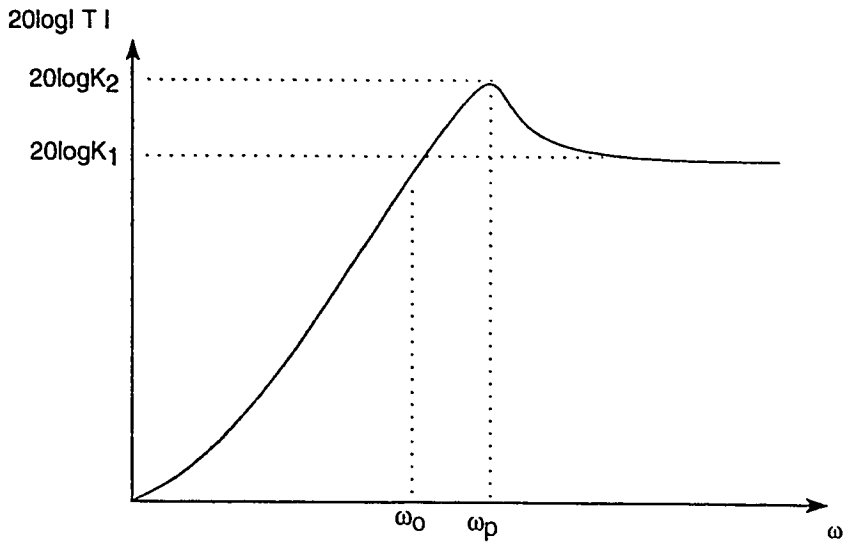

Figure 3.4: Generalized High-Pass Filter Response

High-Pass Filter

The high-pass filter is specified in much the same manner as the low-pass filter. A typical second order active high-pass filter has a gain function as shown in Fig. 3.4. The second order function which realizes a high-pass gain characteristics is given by the following transfer function:

$$T(s) = \frac{a_n s^2}{a_d s^2 + b_d s + c_d} \tag{3.20}$$

and the resulting expression for magnitude is given by

$$|T(j\omega)| = \frac{a_n \omega^2}{\sqrt{(c_d - a_d \omega^2)^2 + (b_d \omega)^2}} \tag{3.21}$$

The parameters a_d, b_d, c_d can be derived directly from equations 3.15, 3.16, and 3.17 respectively, whereas a_n is given by

$$a_n = K_1$$

ω_p and Q are given by equations 3.19 and 3.18 respectively. K_1 is the high-frequency gain of the filter, ($|T(j\infty)| = K_1$) and K_2 is the gain of the filter at $\omega = \omega_p$. In principle, the passband of the high-pass filter extends to $\omega = \infty$. In practice, however, the passband is limited by the finite bandwidth of the active devices and parasitic capacitances.

Band Pass Filter

The function of the band-pass filter is to pass a finite band of frequencies while attenuating both lower and higher frequencies. In general, the band-pass filter response will not be symmetrical and attenuation in the lower and upper passbands will be unequal [33].

A typical second order active bandpass filter has a frequency response as shown in Fig. 3.5. K is the center-frequency gain of the filter. ω_a and ω_b are the cut-off frequencies, that is

$$|T(j\omega_{a,b})| = \frac{K}{\sqrt{2}}$$

The corresponding transfer function for the filter is given by

$$T(s) = \frac{b_n s}{a_d s^2 + b_d s + c_d} \tag{3.22}$$

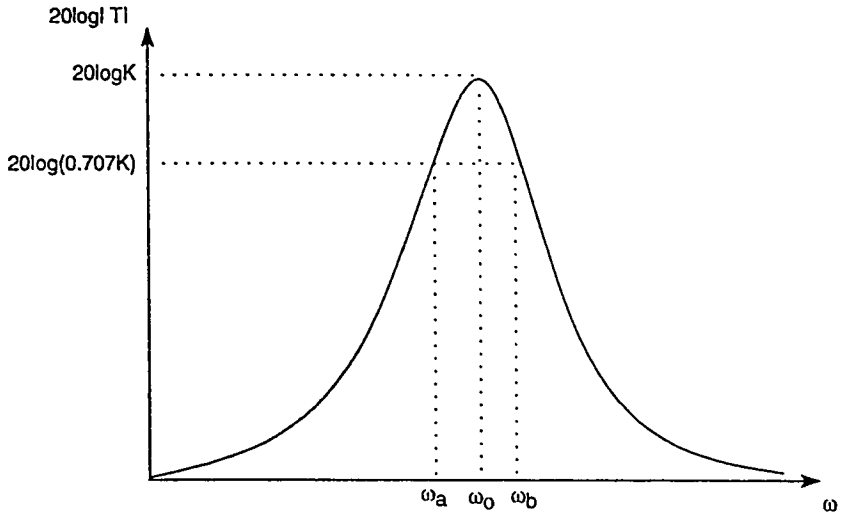

Figure 3.5: Generalized Band-Pass Filter Response

and the resulting expression for magnitude is given by

$$|T(j\omega)| = \frac{b_n\omega}{\sqrt{(c_d - a_d\omega^2)^2 + (b_d\omega)^2}} \tag{3.23}$$

The parameters a_d, b_d, c_d can again be derived directly from equations 3.15, 3.16, and 3.17 respectively by replacing ω_p with ω_o, whereas b_n is given by

$$b_n = \frac{K\omega_o^2}{Q}$$

where

$$Q = \frac{\omega_o}{\omega_b - \omega_a}$$

K is the passband gain of the filter ($|T(j\omega_o)| = K$).

Band Reject Filter

A band-reject filter is used to attenuate a finite band of frequencies while passing both lower and higher frequencies. To achieve a symmetric band-reject gain response as shown in Fig. 3.6, the pole and zero frequencies, ω_p and ω_z, of the filter transfer function must overlap. K is the dc or high-frequency gain, ω_a and ω_b are the cut-off frequencies of the stopband, that is

$$|T(j\omega_{a,b})| = \frac{K}{\sqrt{2}}$$

The corresponding transfer function for the filter is given by

$$T(s) = \frac{a_n s^2 + c_n}{a_d s^2 + b_d s + c_d} \tag{3.24}$$

and the resulting expression for magnitude is given by

$$|T(j\omega)| = \frac{c_n - a_n \omega^2}{\sqrt{(c_d - a_d \omega^2)^2 + (b_d \omega)^2}} \tag{3.25}$$

The parameters a_d, b_d, c_d can derived, as before, directly from equations 3.15, 3.16, and 3.17 respectively, and

$$a_n = K$$

$$c_n = K\omega_z^2$$

where K is the passband gain of the filter ($|T(j0, \infty)| = K$).

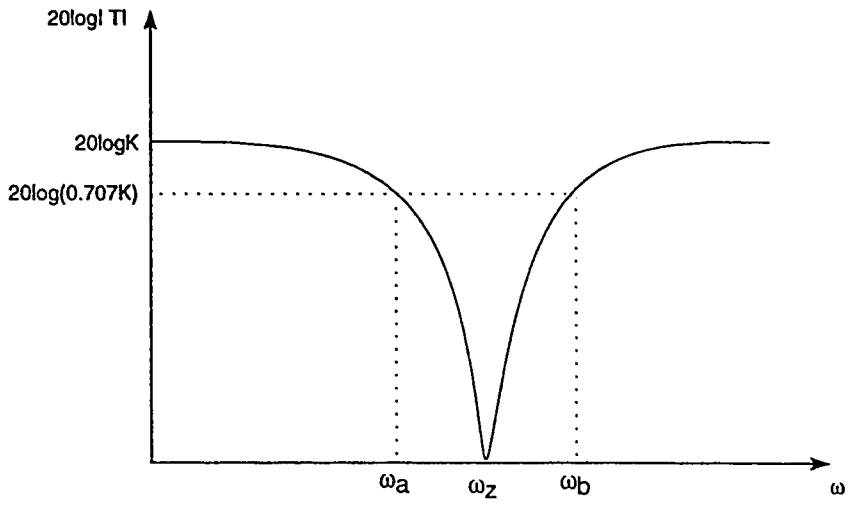

Figure 3.6: Generalized Band-Reject Filter Response

3.5 Conclusions

A new simplified mathematical model has been proposed in the preceeding sections. Most curve-fitting procedures require minimal effort since reasonably accurate seed values are readily obtainable by visual inspection on the plotted data. The mathematical funtions used to model the system response require experimental measurements of trivial nature.

The choice of fitting functions suits the desired accuracy while maintaining a very small number of coefficients. This has been made possible by selecting mathematical functions which represent the natural circuit reponse.

The proposed model is valid for multi-tone input with arbitrary amplitudes and no significant assumptions have been made which undermine the accuracy or gen-

erality of the model.

Intermodulation analysis using the proposed model is fairly easy and can be implemented on a personal computer.

Chapter 4

Results and Discussion

4.1 Introduction

A new model has been proposed in the previous chapter in an attempt to rectify some of the disadvantages of the existing models. Any proposition would be untenable in the absence of practical results. Experimental measurements and the simulation results based on this model are presented in this chapter.

Several circuits were constructed for the verification of the proposed model. The results of four circuits are presented here to demonstrate the validity of the model. The selection of circuits represents the basic categories of frequency responses of communication systems, that are, low-pass, high-pass, band-pass and band-reject.

Second-order filter sections built around a single operational amplifier have been used widely in the literature to study the nonlinear behaviour of systems [1, 2, 14,

17, 18, 21, 22, 34]. The circuits presented for model validation are single-amplifier biquad (SAB) [35] filters constructed using a single operational amplifier and passive elements.

4.2 Experimental Considerations

Some important experimental requisites need to be explained before presenting the actual results. The signal sources should have minimal harmonic content. Ideally, the amplitude of most significant harmonic should be at least -80dB below that of the fundamental frequency. This may require operation of the signal source at low amplitudes.

An ideal summation circuit must be used at the input to form the multi-tone sinusoidal input. Any distortion in the summation circuit is bound to undermine the accuracy of results. The amplitudes of input sinusoids must be measured from a spectrum analyzer in order to obtain a correct value.

A buffer circuit may be required between the input signal sources and the circuit under test. The buffer would prevent loading of the sources by the circuit, hence ensuring the desired value of input amplitude at all frequencies. Moreover, the buffer will isolate the signal sources from the effect of distorted signal being fed back at the input of the test system.

A proposed experimental set-up is shown in Fig. 4.1. The signal sources are

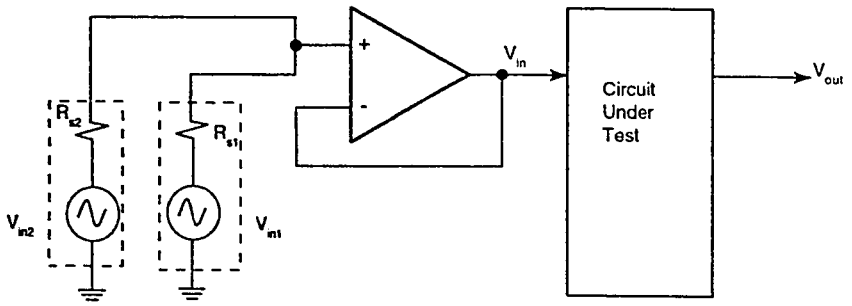

Figure 4.1: Proposed Experimental Setup for Two-tone Intermodulation Measurement

coupled together at the input of the buffer section. The output of the buffer is then fed to the input of the filter circuit under test.

4.3 Measurement of Input-Output Characteristics

The first step in determining the equivalent mathematical model of a nonlinear system is the measurement of its input-output characteristics at a nominal frequency. The nominal frequeny ω_{nom} is chosen such that the magnitude of filter transfer function is at its maximimum value, that is $|T(j\omega)|_{max}$.

The onset of nonlinearity in active filters is primarily a function of the supply voltages of the operational amplifiers. The value of supply voltages has been chosen to deliberately introduce a measureable amount of nonlinearity in the system.

The choice of order of power series approximation need to be addressed since it can significantly affect the predicted spectrum component levels.

During the course of verification it was found that the input-output characteristics of a practical operational amplifier are not an exact antisymmetric function of the input voltage. This observation was verified by the presence of even order harmonics of the input sinusoids, at the output, for single-tone measurements.

To obtain an accurate power series approximation of the input-output characteristics, it was found necessary to measure the output for positive and negative input voltages separately. The amplitude characteristics of the circuits were, therefore, determined by measuring the peak voltages for negative and postive swing of input voltage.

The resulting mathematical approximation therefore contains both odd and even order terms. A power series approximation (Equation 3.4) upto fifth order was found to be sufficient to represent the characteristics accurately, that is

$$V_{out} = \sum_{i=1}^{5} k_i V_{in}^i \tag{4.1}$$

where

$$V_{in} = V_1 + V_2$$

The input-output measurements were recorded until the onset of severe nonlinearity where the output waveform could be observed to be clipped. Mathematically this condition can be expressed as,

$$\frac{dV_{out}}{dV_{in}} \approx 0$$

It has been ensured that the relative root-mean-square error in any of the curve-fitting procedures does not exceed 0.01.

4.4 Measurement of Harmonics and Intermodulation Products

Since the two-tone case in normally considered to be the most important [1. 36], the active filter under test was excited simultaneously by a sum of two sinusoids. The verification could be extended to a larger number of input signals but it would become increasingly difficult to select frequencies such that the harmonics and intermodulation products do not overlap.

The input sinusoids were chosen to be in the passband of the filter which represents a realistic situation. The carrier amplitudes have been selected so as to avoid severe nonlinearity while introducing a measureable quantity of distortion.

The amplitudes of harmonics and intermodulation products at the output of nonlinear system were measured using a spectrum analyzer. The measurements were carried out only for frequency components which had an amplitude greater than -70dB with reference to the carrier output [37] which is a realistic assumption for commercial color television broadcast signal. The range correponds to less than 0.1% in the absolute terms.

The frequency range selected for measurements was restricted to 40kHz since

the finite bandwidth of the operational amplifier and the stray capacitances tend to affect the accuracy of results beyond this frequency.

The resolution of visual measurement from the spectrum analyzer was 0.5kHz on the frequency scale and $1dBV_{rms}$ on the amplitude scale.

The experimental results for various combinations of input frequencies and amplitudes are reported. Absolute error between the measured values of amplitudes and those predicted by the proposed model, has been shown in tabular form. All signal amplitudes are expressed in dBV_{rms} and all frequencies are represented in kHz.

4.5 Experimental Results

The experimental results of four sample circuits are presented below. The input-output characteristics are represented in graphical form. A closed form expression in terms of power series has been obtained by curve-fitting of $V_{in} \sim V_{out}$ measured at a nominal frequency. The output frequency spectrum for some sample inputs have been included for graphical representation of the amplitudes of the harmonics and intermodulation products.

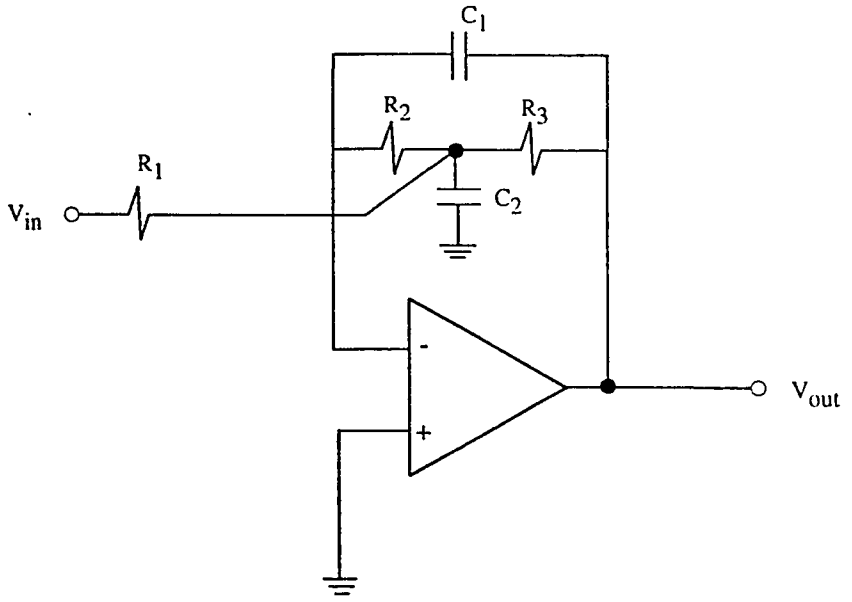

Figure 4.2: Second-Order Low-Pass Filter Circuit

4.5.1 Low Pass Filter

The low-pass filter circuit is shown in Fig. 4.2. The design parameters are as follows: $f_o = 11\text{kHz}$, $Q = \frac{1}{\sqrt{2}}$. The value of quality factor Q has been selected so as to yield a maximally flat frequency response [31].

The transfer function of the filter in terms of circuit parameters is given by:

$$T(s) = -\frac{\frac{1}{R_1 R_2 C_1 C_2}}{s^2 + \frac{R_1 R_2 + R_2 R_3 + R_1 R_3}{R_1 R_2 R_3 C_2} s + \frac{1}{R_2 R_3 C_1 C_2}}$$

The component values calculated for the required design specifications are:

$R_1 = 100\Omega$, $R_2 = 700\Omega$, $R_3 = 700\Omega$

$C_1 = 2.2\text{nF}$, $C_2 = 10\text{nF}$

The frequency response of the filter is shown in Fig. 4.3.

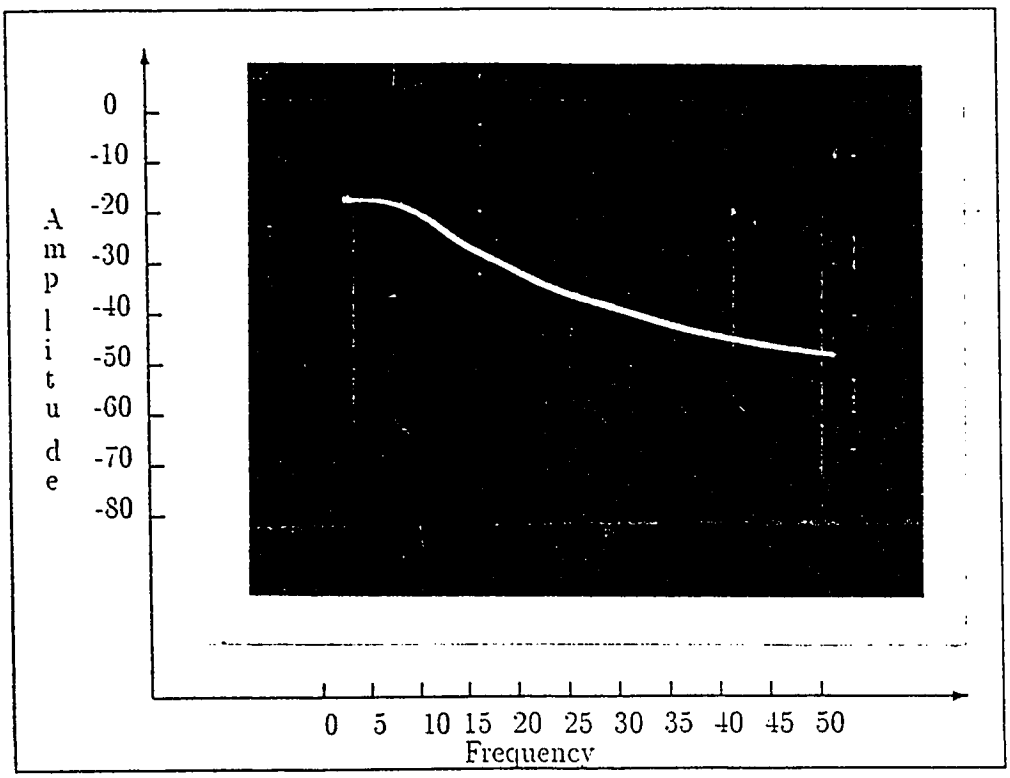

Figure 4.3: Frequency Response of the Low-Pass Filter f_{nom}=100Hz Amplitude: dBV_{rms}; Frequency: kHz

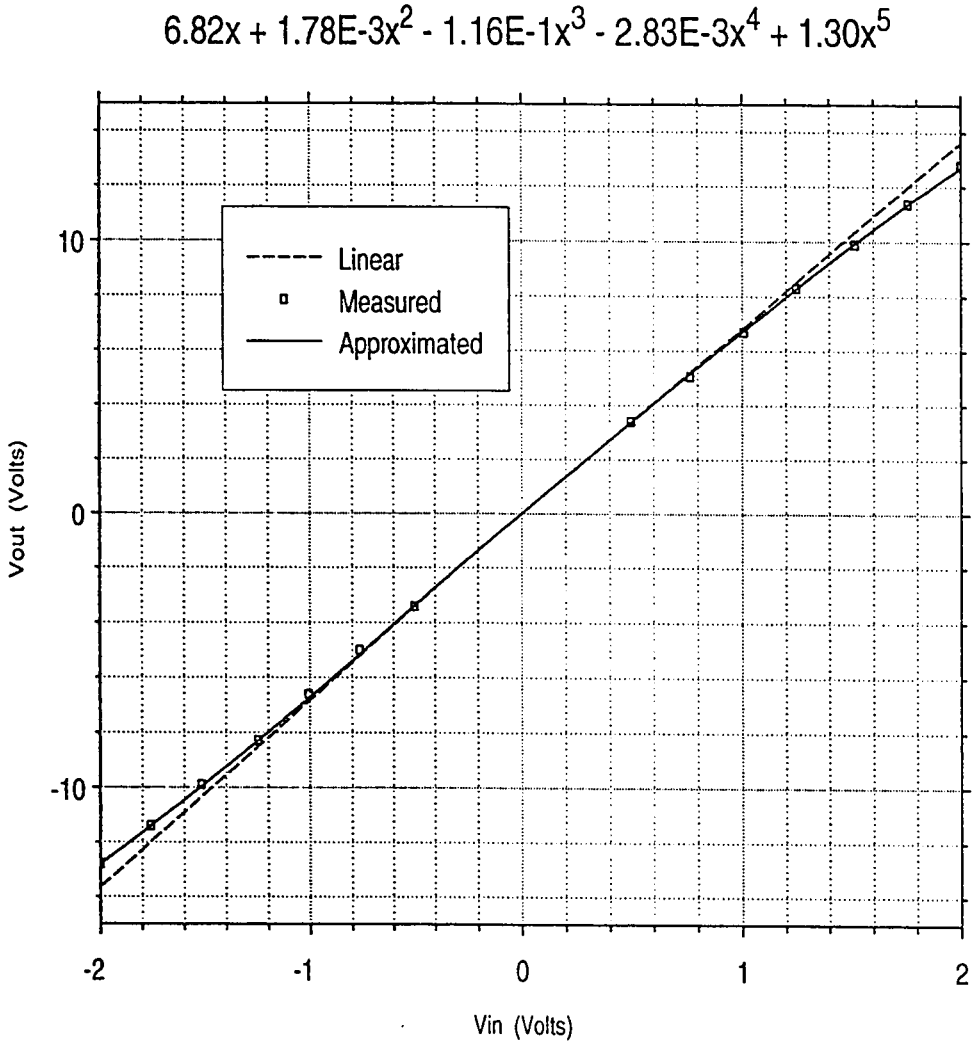

Figure 4.4: Input-Output Characteristics of Low-Pass Filter measured f_{nom}

Input-Output Characteristics

The supply voltages were fixed at ±10 Volts and the nominal frequency for measurement of input-output characteristics (Fig. 4.4) was chosen to be $f_{nom} = 100$Hz. The coefficients of power series approximation (Equation 4.1) of these characteristics obtained by curve-fitting are given in Table 4.1.

k_1	6.82
k_2	1.78E-3
k_3	-1.16E-1
k_4	-2.83E-3
k_5	1.30E-3

Table 4.1: Power Series Coefficients for Input-Ouput Characteristics of Low-Pass Filter

	a_n	b_n	c_n	a_d	b_d	c_d
$H(j\omega)$	0	0	4.77E9	1	9.77E4	4.77E9
$G(j\omega)$	0	0	2.38E9	1	9.09E4	4.87E9

Table 4.2: Prefilter and Postfilter Curve-fit Coefficients for Low-Pass Filter

Prefilter and Postfilter Blocks

The curve-fitting coefficients obtained for the prefilter $H(j\omega)$ and postfilter $G(j\omega)$ functions (Equation 3.13) for the low-pass filter are shown in Table 4.2.

Harmonics and Intermodulation Products

The measured(V_M) and predicted(V_P) amplitudes for various sets of input frequencies and amplitudes are tabulated below. The absolute error(E) has also been calculated.

$$E = |V_M - V_P|$$

The measured and predicted amplitudes of harmonics and intermodulation products for low-pass filter are given in Tables 4.3, 4.4, and 4.5. A sample screen image of the spectrum analyzer for measurements is shown in Fig. 4.5.

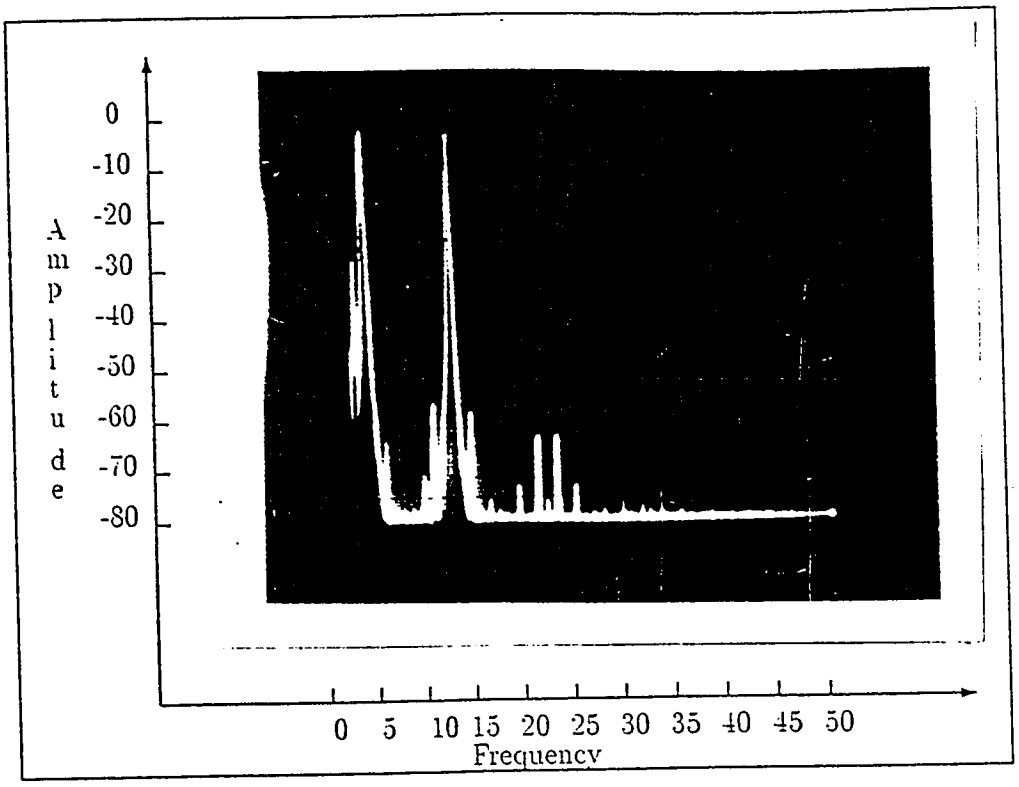

Figure 4.5: Intermodulation Distortion in Low-Pass Filter (f_1=5kHz f_2=11kHz) Amplitude: dBV_{rms}; Frequency: kHz

Harmonic IMP	Freq. (kHz)	V_1= -15dBV V_2= -15dBV			V_1=-18dBV V_2=-18dBV			V_1=-20dBV V_2=-20dBV		
		V_M	V_P	E	V_M	V_P	E	V_M	V_P	E
f_1	1	2	2.1	0.1	-1	-0.7	0.3	-3	-2.7	0.3
$3f_1$	3	-59	-56.1	2.9	-66	-64.9	1.1	-72	-70.8	1.2
$-2f_1+f_2$	8	-51	-49.8	1.1	-60	-58.6	1.3	-64	-64.6	0.6
f_2	10	-1	-0.1	0.8	-60	-58.6	1.3	-64	-64.6	0.6
$2f_1+f_2$	12	-54	-52.5	1.5	-62	-61.4	0.6	-66	-67.3	1.3
$-f_1+2f_2$	19	-60	-60.9	0.9	-67	-69.8	2.8	-73	-75.7	2.7

Table 4.3: Amplitudes of Harmonics and Intermodulation Products (dBV_{rms}) for Low-Pass Filter with f_1=1kHz and f_2=10kHz

Harmonic IMP	Freq. (kHz)	V_1= -18dBV V_2= -20dBV			V_1=-20dBV V_2=-18dBV		
		V_M	V_P	E	V_M	V_P	E
$-2f_1+f_2$	1	-64	-60.7	3.3	-72	-73.8	1.8
f_1	5	-2	-0.9	1.1	-4	-2.9	1.1
f_2	11	-7	-5.8	1.2	-4	-3.8	0.2
$3f_1$	15	-72	-71.9	0.1	-75	-77.9	2.9
$-f_1+2f_2$	17	-72	-73.8	1.8	-70	-71.7	1.7

Table 4.4: Amplitudes of Harmonics and Intermodulation Products (dBV_{rms}) for Low-Pass Filter with f_1=5kHz and f_2=11kHz

Harmonic IMP	Freq. (kHz)	V_1= -15dBV V_2= -15dBV			V_1=-18dBV V_2=-18dBV			V_1=-20dBV V_2=-20dBV		
		V_M	V_P	E	V_M	V_P	E	V_M	V_P	E
f_1	2	1	2.1	1.1	-2	-0.8	1.2	-3	-2.7	0.3
$-2f_1+f_2$	5	-51	-48.3	2.7	-60	-57.1	2.9	-66	-63.8	2
$3f_1$	6	-59	-56.5	2.5	-68	-65.3	2.7	-68	-71.2	3.2
f_2	9	1	2.1	1.1	-2	-0.7	1.3	-3	-2.7	1.3
$2f_1+f_2$	13	-56	-52.8	3.2	-68	-65.3	2.7	-68	-71.2	3.2
$-f_1+2f_2$	16	-60	-57.1	2.9	-64	-65.9	1.9	-75	-71.9	3.1

Table 4.5: Amplitudes of Harmonics and Intermodulation Products (dBV_{rms}) for Low-Pass Filter with f_1=2kHz and f_2=9kHz

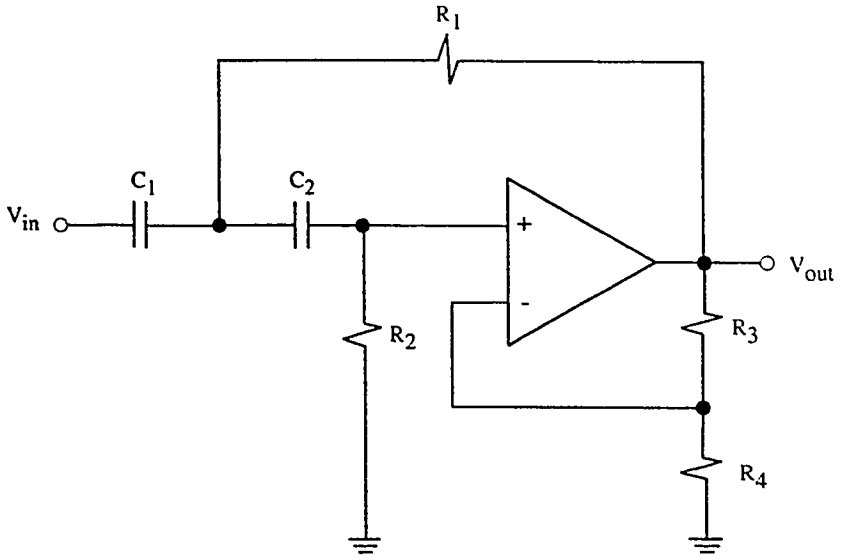

Figure 4.6: Second-Order High-Pass Filter Circuit

4.5.2 High Pass Filter

The high-pass filter circuit is shown in Fig. 4.6. The design parameters are as follows: $f_o = 10\text{kHz}$, $Q = \frac{1}{\sqrt{2}}$. The value of quality factor Q has been selected so as to yield a maximally flat frequency response.

The transfer function of the filter in terms of circuit parameters is given by:

$$T(s) = \frac{1}{a} \frac{s^2}{s^2 + \frac{R_1R_1C_1 - R_2R_3C_2}{R_1R_2R_4C_1C_2}s + \frac{1}{R_1R_2C_1C_2}}$$

where

$$a = \frac{R_4}{R_3 + R_4}$$

The component values calculated for the required design specifications are:

$R_1 = 1.948\text{K}\Omega$, $R_2 = 1.3\text{K}\Omega$, $R_3 = 10\text{K}\Omega$, $R_4 = 12.88\text{K}\Omega$

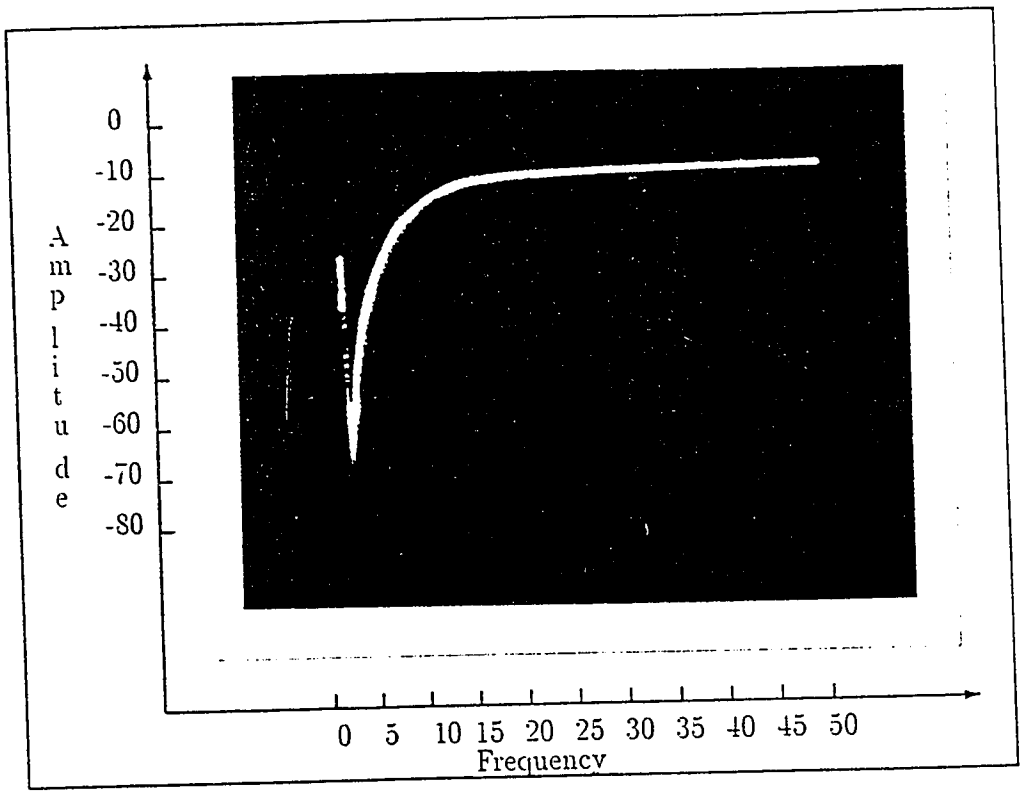

Figure 4.7: Frequency Response of the High-Pass Filter f_{nom}=40kHz Amplitude: dBV_{rms}; Frequency: kHz

$C_1 = 10\text{nF}$, $C_2 = 10\text{nF}$

The frequency response of the high-pass filter is shown in Fig. 4.7.

Input-Output Characteristics

The supply volatges were fixed at ± 5 Volts and the nominal frequency for measurement of input-output characteristics (Fig. 4.8) was chosen to be $f_{nom} = 40\text{kHz}$. The coefficients of power series approximation (Equation 4.1) of the input-output characteristics obtained by curve-fitting are as shown in Table 4.6.

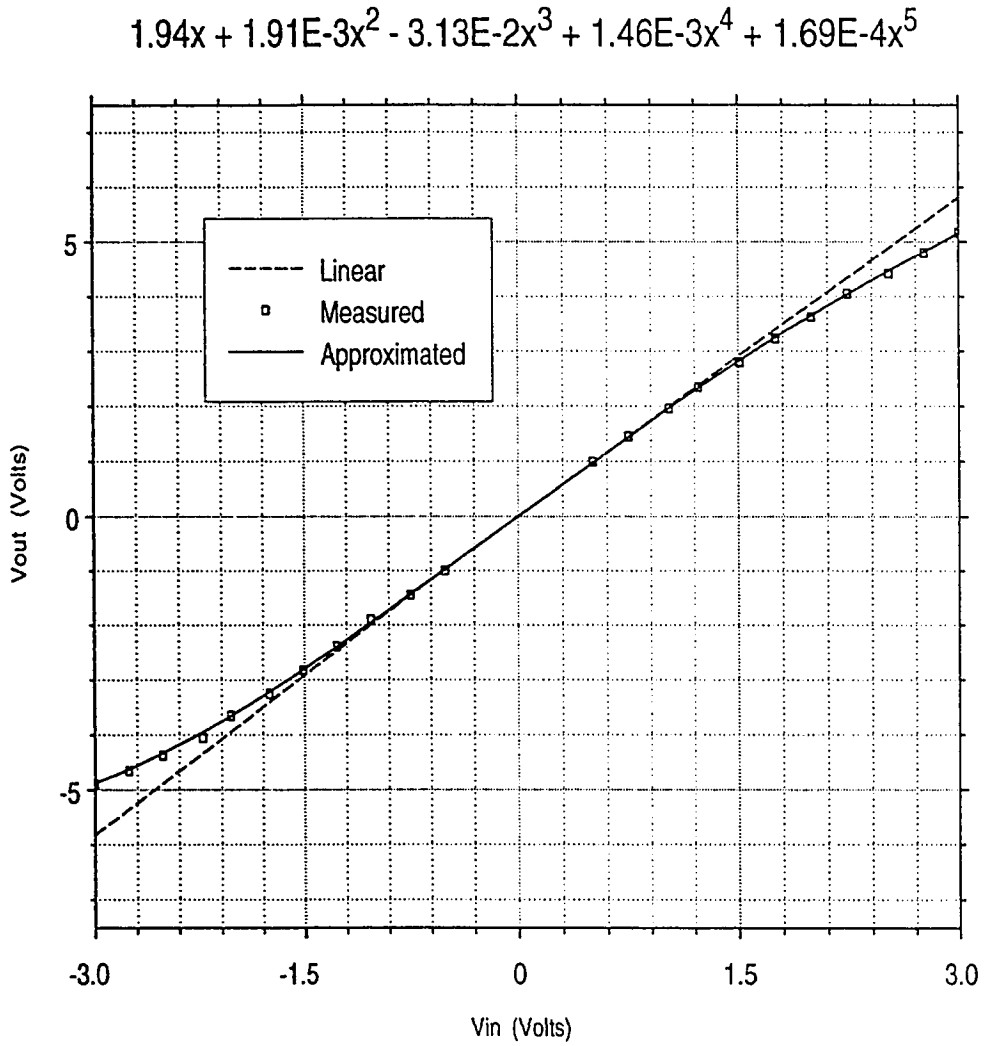

Figure 4.8: Input-Output Characteristics of High-Pass Filter measured at f_{nom}

k_1	1.94
k_2	1.91E-3
k_3	-3.13E-2
k_4	1.46E-3
k_5	1.69E-4

Table 4.6: Power Series Coefficients for Input-Ouput Characteristics of High-Pass Filter

	a_n	b_n	c_n	a_d	b_d	c_d
$H(j\omega)$	1	0	0	1	8.88E4	3.94E9
$G(j\omega)$	0.42	0	0	1	9.09E4	4.13E9

Table 4.7: Prefilter and Postfilter Curve-fit Coefficients for High-Pass Filter

Harmonic IMP	Freq. (kHz)	V_1= -15dBV V_2= -15dBV			V_1=-11dBV V_2=-11dBV			V_1=-11dBV V_2=-15dBV		
		V_M	V_P	E	V_M	V_P	E	V_M	V_P	E
$2f_1 - f_2$	7	-	-	-	-66	-64.5	1.5	-	-	-
f_1	15	-10	-10.1	0.1	-6	-6.2	0.2	-6	-6.2	0.2
f_2	23	-10	-9.4	0.6	-5	-5.5	0.5	-10	-9.5	0.5
$-f_1 + 2f_2$	31	-	-	-	-60	-56.4	3.5	-66	-64.3	1.7
$f_1 + f_2$	38	-	-	-	-66	-64.5	1.5	-71	-74.4	3.4

Table 4.8: Amplitudes of Harmonics and Intermodulation Products (dBV_{rms}) for High-Pass Filter with f_1=15kHz and f_2=23kHz

Prefilter and Postfilter Blocks

The curve-fitting coefficients obtained for the prefilter $H(j\omega)$ and postfilter $G(j\omega)$ functions (Equation 3.21) for the high-pass filter are shown in Table 4.7.

Harmonics and Intermodulation Products

The measured and predicted amplitudes of harmonics and intermodulation products for high-pass filter are given in Tables 4.8. 4.9. and 4.10. A sample screen image of the spectrum analyzer for measurements is shown in Fig. 4.9. The absence of a measurement in the tables indicates that the amplitude was less than -70dB with respect to the carrier level at the output.

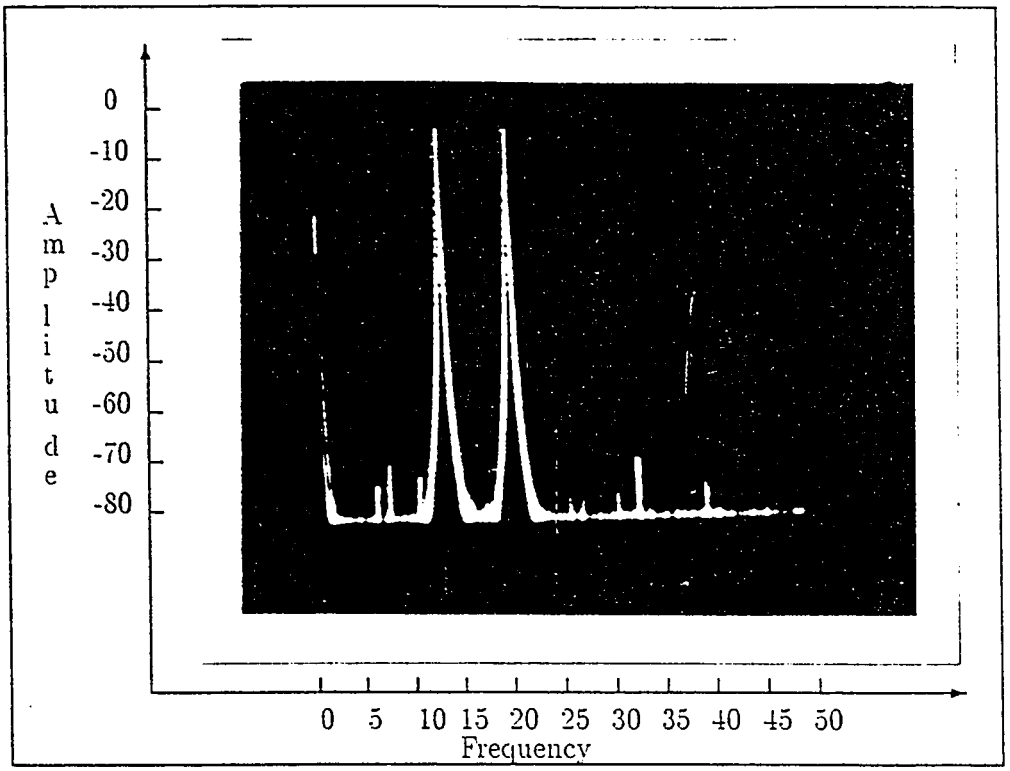

Figure 4.9: Intermodulation Distortion in High-Pass Filter (f_1=13kHz f_2=20kHz) Amplitude: dBV_{rms}; Frequency: kHz

Harmonic IMP	Freq. (kHz)	V_1= -15dBV V_2= -15dBV			V_1=-10dBV V_2=-10dBV		
		V_M	V_P	E	V_M	V_P	E
f_1	10	-13	-12.5	0.5	-7	-7.6	0.6
f_2	19	-10	-9.6	0.4	-4	-4.7	0.7
$-f_1+2f_2$	28	-	-	-	-59	-56.1	2.9
f_1+f_2	29	-	-	-	-71	-69.3	1.7
$3f_1$	30	-	-	-	-70	-71.4	1.4
$2f_2$	38	-	-	-	-74	-71.8	2.2
$2f_1+f2$	39	-	-	-	-61	-58.9	2.1

Table 4.9: Amplitudes of Harmonics and Intermodulation Products for High-Pass Filter with f_1=10kHz and f_2=19kHz

Harmonic IMP	Freq. (kHz)	V_1= -15dBV V_2= -15dBV			V_1=-11dBV V_2=-11dBV		
		V_M	V_P	E	V_M	V_P	E
$2f_1 - f_2$	6	-	-	-	-70	-68	2
$-f_1 + f_2$	7	-	-	-	-75	-77.1	2.1
f_1	13	-10	-10.7	0.7	-6	-6.8	0.8
f_2	20	-6	-5.7	0.3	-6	-5.7	0.3
$2f_1$	26	-	-	-	-77	-75.1	1.9
$-f_1 + 2f_2$	27	-	-	-	-60	-57.2	2.8
$f_1 + f_2$	33	-	-	-	-73	-69.7	3.3
$3f_1$	39	-	-	-	-60	-60	0

Table 4.10: Amplitudes of Harmonics and Intermodulation Products (dBV_{rms}) for High-Pass Filter with f_1=13kHz and f_2=20kHz

4.5.3 Band Pass Filter

The band-pass filter circuit is shown in Fig. 4.10. The design parameters for the filter are: $f_c = 20$kHz and $Q = 5$. The cut-off frequencies, therefore, are $f_a = 18$kHz and $f_b = 22$kHz.

The transfer function of the filter in terms of circuit parameters is given by:

$$T(s) = -\frac{\frac{1}{R_2C_1}s}{s^2 + \frac{R_1(C_1+C_2)}{R_1R_2C_1C_2}s + \frac{1}{R_1R_2C_1C_2}}$$

The component values calculated for the required design specifications are:

$R_1 = 79.5\Omega$, $R_2 = 7.95\text{K}\Omega$

$C_1 = 10$nF , $C_2 = 10$nF

The frequency reponse of the band-pass filter is shown in Fig. 4.11

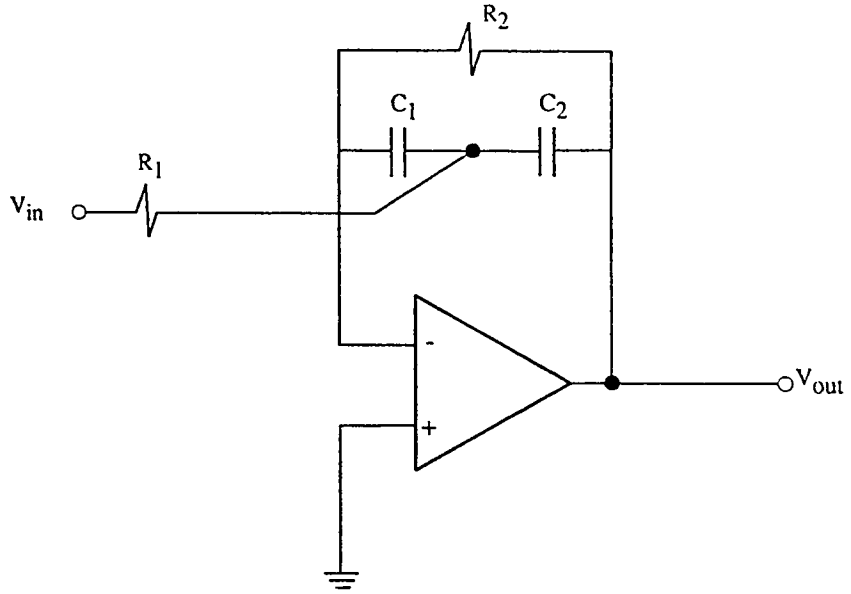

Figure 4.10: Second-Order Band-Pass Filter Circuit

Input-Output Characteristics

The supply volatges were fixed at ±15 Volts and the nominal frequency for measurement of input-output characteristics (Fig. 4.12) is selected to be the center frequency of the bandpass filter, that is $f_{nom} = f_c = 20$kHz. The coefficients of power series approximation (Equation 4.1) of the input-output characteristics obtained by curve-fitting are shown in Table 4.11.

Prefilter and Postfilter Blocks

The curve-fitting coefficients obtained for the prefilter $H(j\omega)$ and postfilter $G(j\omega)$ functions (Equation 3.23) for the band-pass filter are given in Table 4.12.

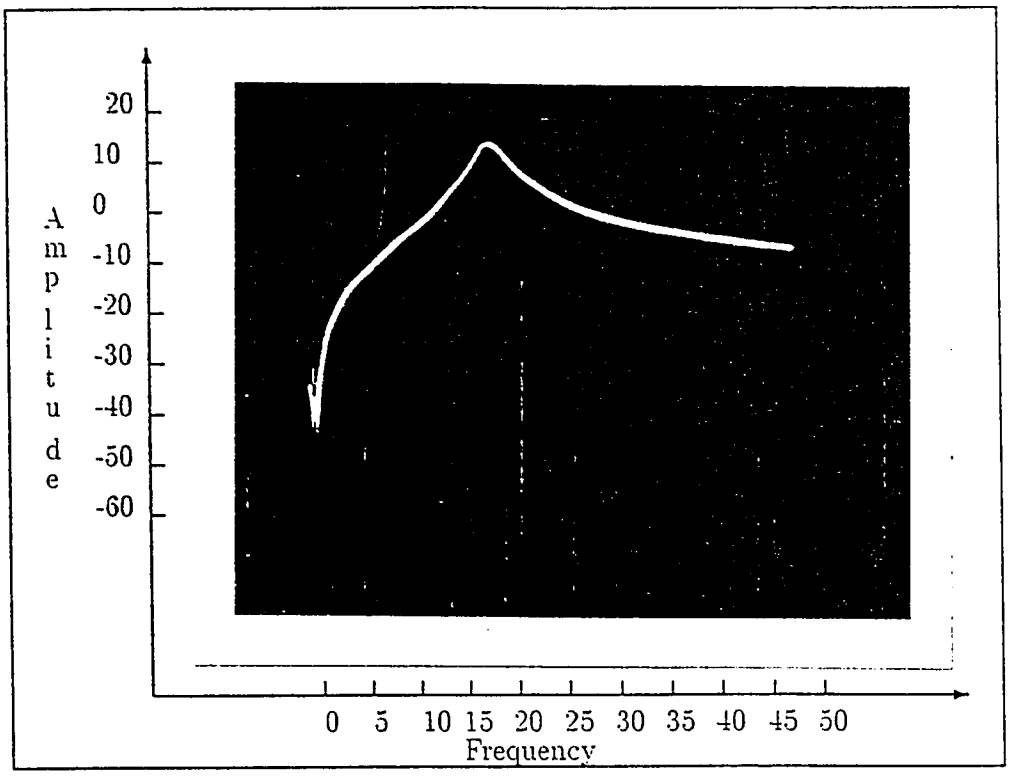

Figure 4.11: Frequency Response of the Band-Pass Filter f_{nom}=20kHz Amplitude: dBV_{rms}; Frequency: kHz

k_1	45.10
k_2	2.38
k_3	-29.4
k_4	13
k_5	-35.93

Table 4.11: Power Series Coefficients for Input-Ouput Characteristics of Band-Pass Filter

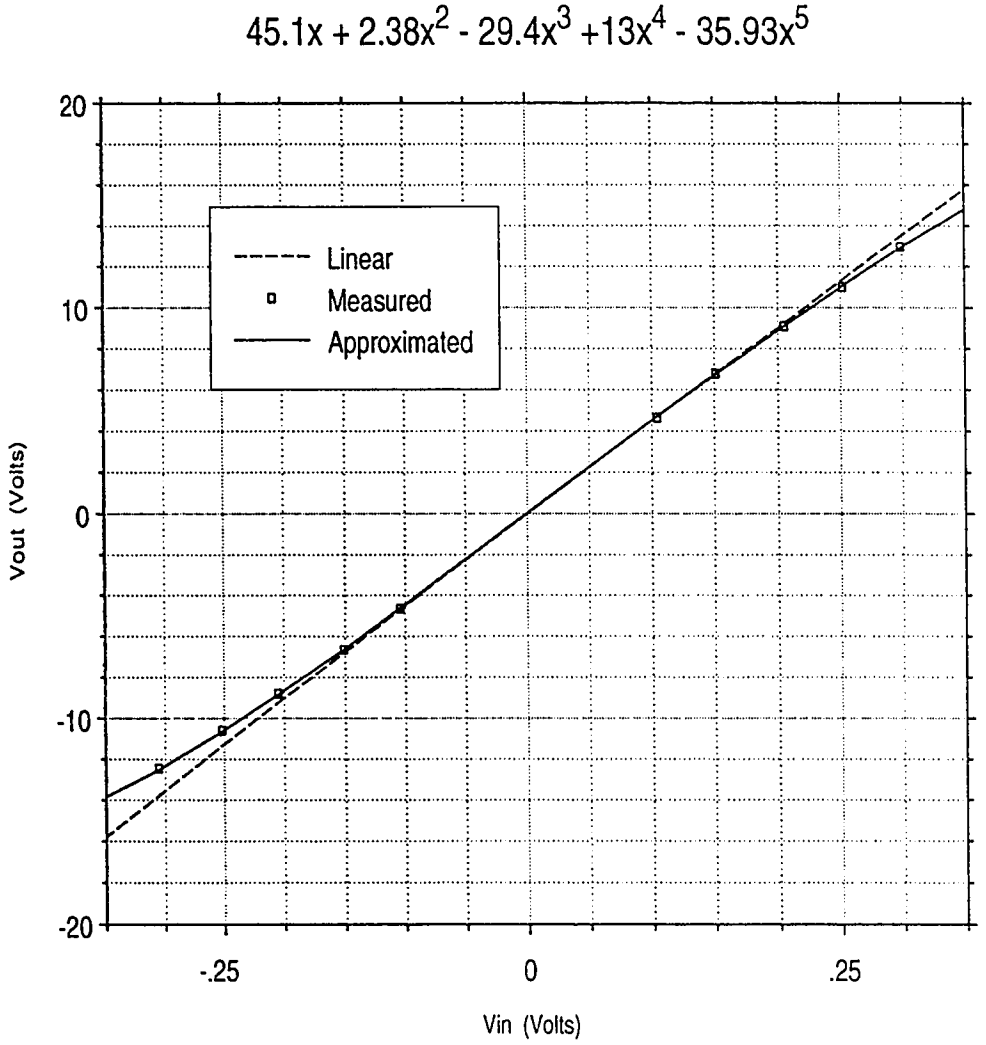

Figure 4.12: Input-Output Characteristics of Band-Pass Filter measured at f_{nom}

	a_n	b_n	c_n	a_d	b_d	c_d
$H(j\omega)$	0	2.51E4	0	1	2.51E4	1.58E10
$G(j\omega)$	0	4.63E4	0	1	3.56E4	1.58E10

Table 4.12: Prefilter and Postfilter Curve-fit Coefficients for Band-Pass Filter

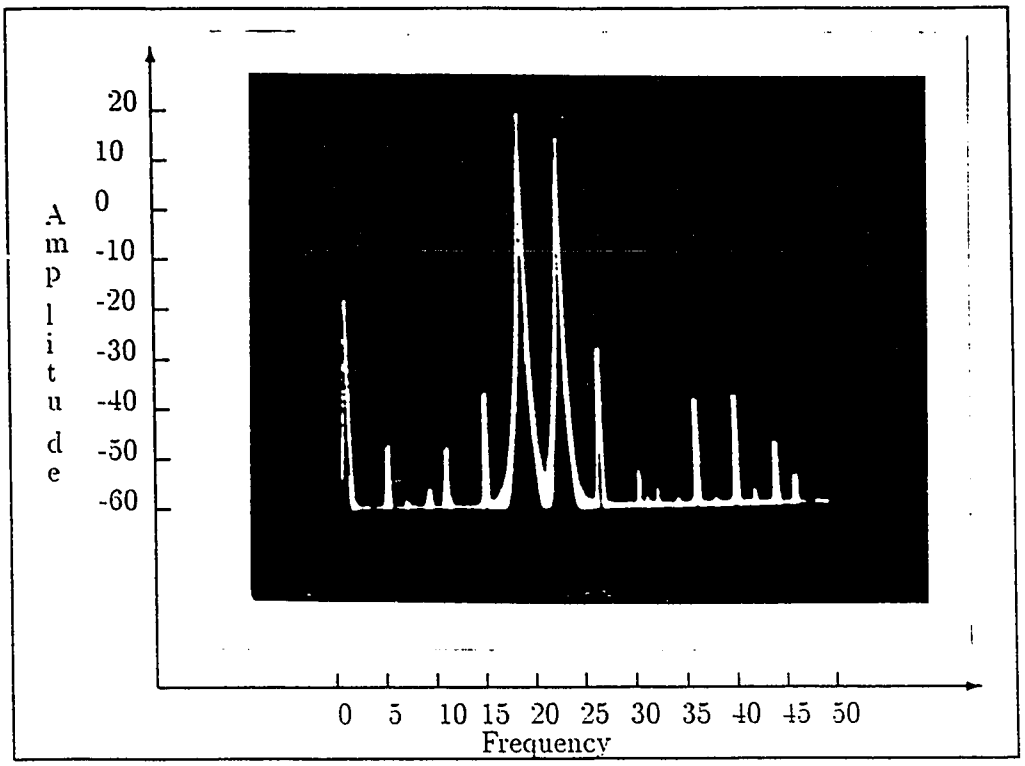

Figure 4.13: Intermodulation Distortion in Band-Pass Filter (f_1=18kHz f_2=22kHz) Amplitude: dBV_{rms}; Frequency: kHz

Harmonics and Intermodulation Products

The measured and predicted amplitudes of harmonics and intermodulation products for band-pass filter are shown in Tables 4.13, 4.14, and 4.15. A sample screen image of the spectrum analyzer for measurements is shown in Fig. 4.13.

Harmonic IMP	Freq. (kHz)	V_1= -21dBV V_2= -21dBV			V_1=-24dBV V_2=-24dBV		
		V_M	V_P	E	V_M	V_P	E
$-f_1+f_2$	4	-50	-46.7	3.3	-56	-54.7	1.3
$-2f_1+2f_2$	8	-61	-59.4	1.6	-	-	-
$3f_1-2f_2$	10	-	-	-	-	-	-
$2f_1-f_2$	14	-31	-28.4	2.6	-40	-38.2	1.8
f_1	18	10	9.6	0.4	8	6.9	1.1
f_2	22	9	9.9	0.9	5	7.1	2.1
$-f_1+2f_2$	26	-29	-25.8	3.2	-38	-35.6	2.3
$-2f_1+3f_2$	30	-57	-58.1	1.1	-70	-73.1	3.1
$3f_1-f_2$	32	-59	-58.8	2.2	-	-	-
$2f_1$	36	-43	-40.3	2.7	-	-	-

Table 4.13: Amplitudes of Harmonics and Intermodulation Products (dBV_{rms}) for Band-Pass Filter with f_1=18kHz and f_2=22kHz

Harmonic IMP	Freq. (kHz)	V_1= -21dBV V_2= -21dBV			V_1=-24dBV V_2=-24dBV		
		V_M	V_P	E	V_M	V_P	E
$-2f_1+2f_2$	4	-60	-61.4	1.4	-	-	-
$3f_1-2f_2$	15	-45	-49.3	4.3	-62	-64.3	2.3
$2f_1-f_2$	17	-16	-18.8	2.8	-6	-6.8	0.8
f_1	19	12	10.8	1.2	10	8.2	1.8
f_2	21	9	10.8	1.8	7	8.2	1.2
$-f_1+2f_2$	23	-16	-18	2	-30	-28.1	1.9
$-2f_1+3f_2$	25	-45	-47.5	2.5	-64	-62.5	1.5
$3f_1-f_2$	36	-56	-53.5	2.5	-	-	-
$2f_1$	38	-40	-37.1	2.9	-46	-46	0

Table 4.14: Amplitudes of Harmonics and Intermodulation Products (dBV_{rms}) for Band-Pass Filter with f_1=19kHz and f_2=21kHz

Harmonic IMP	Freq. (kHz)	V_1= -21dBV V_2= -21dBV			V_1=-24dBV V_2=-21dBV		
		V_M	V_P	E	V_M	V_P	E
$-f_1+f_2$	2	-54	-54.8	0.8	-54	-54.3	0.3
$-2f_1+2f_2$	4	-70	-69.3	0.7	-70	-69.3	0.7
$2f_1-f_2$	16	-26	-26.5	6.5	-28	-29.2	1.2
f_1	18	11	9.7	1.3	8	6.5	1.5
f_2	20	9	8.6	0.4	11	11.61	0.6
$-f_1+2f_2$	22	-22	-23.8	1.8	-20	-20.8	0.8
$-2f_1+3f_2$	24	-53	-56.6	3.6	-50	53.6	3.6
$3f_1-f_2$	34	-57	-59.2	2.2	-62	-65.2	3.2
$2f_1$	36	-42	-41.2	0.8	-46	-45.4	0.6
f_1+f_2	38	-40	-37.9	2.1	-	-	-

Table 4.15: Amplitudes of Harmonics and Intermodulation Products (dBV_{rms}) for Band-Pass Filter with f_1=18kHz and f_2=20kHz

4.5.4 Band Reject Filter

The band-reject filter circuit is shown in Fig. 4.14. The design parameters for the filter are: $f_c = 20$kHz and $Q = 5$.

The transfer function of the filter in terms of circuit parameters is given by:

$$T(s) = a\frac{s^2 + \frac{1}{R_1R_2C_1C_2}}{s^2 + \left(\frac{1}{R_1C_2} + \frac{1}{R_2C_1}\right)s + \frac{1}{R_1R_2C_1C_2}}$$

where

$$a = \frac{R_4}{R_3 + R_4}$$

The component values calculated for the required design specifications are:

$R_1 = 79.5\Omega$, $R_2 = 7.95\text{K}\Omega$, $R_3 = 1\text{K}\Omega$, $R_4 = 50\text{K}\Omega$

$C_1 = 10$nF , $C_2 = 10$nF

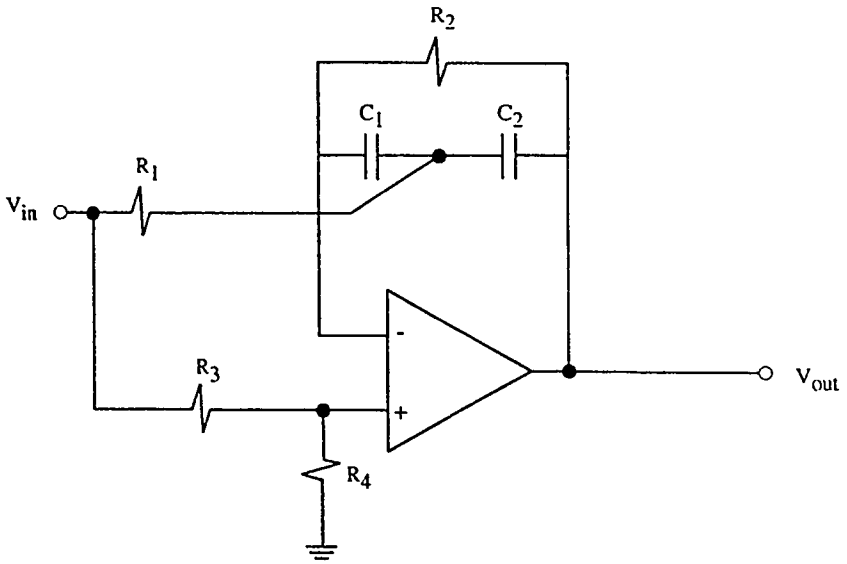

Figure 4.14: Second-Order Band-Reject Filter Circuit

The frequency response of the band-reject filter is shown in Fig. 4.15.

Input-Output Characteristics

The supply volatges were fixed at ±3 Volts and the nominal frequency for measurement of input-output characteristics (Fig. 4.16) is f_{nom} = 1kHz. The coefficients of power series approximation (Equation 4.1) of the input-output characteristics obtained by curve-fitting are as given in Table 4.16.

Prefilter and Postfilter Blocks

The curve-fitting coefficients obtained for the prefilter $H(j\omega)$ and postfilter $G(j\omega)$ functions (Equation 3.25) for the high-pass filter are shown in Table 4.17.

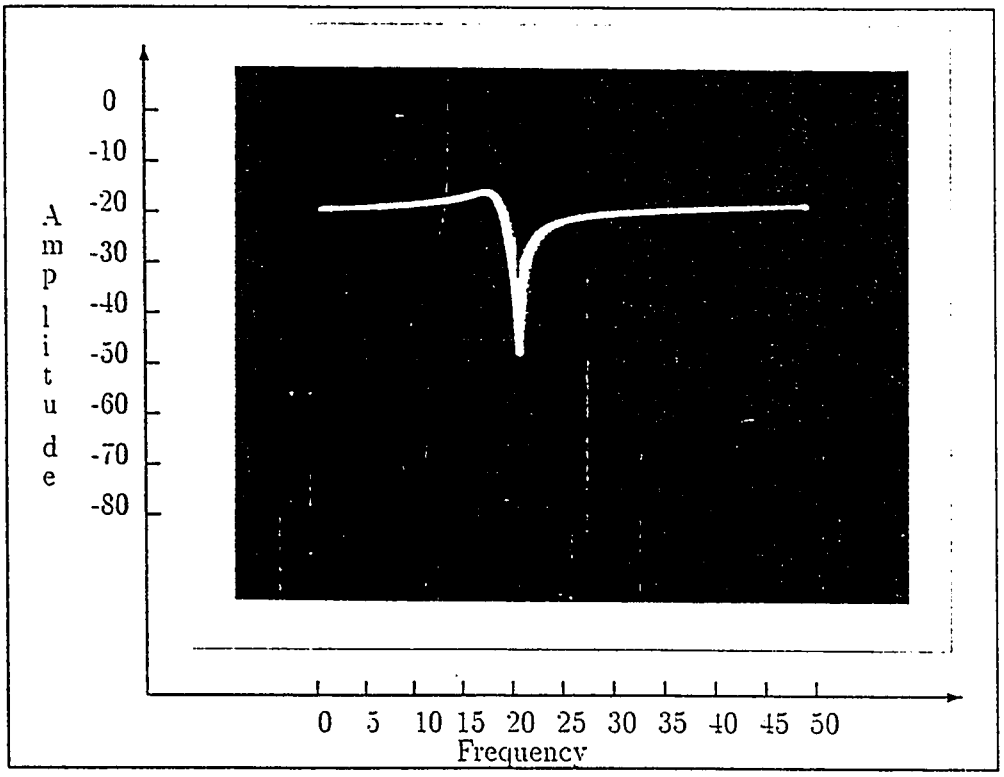

Figure 4.15: Frequency Response of the Band-Reject Filter f_{nom}=1kHz Amplitude: dBV_{rms}; Frequency: kHz

k_1	0.99
k_2	2.95E-4
k_3	-5.9E-3
k_4	3.08E-4
k_5	3.27E-4

Table 4.16: Power Series Coefficients for Input-Ouput Characteristics of Band-Reject Filter

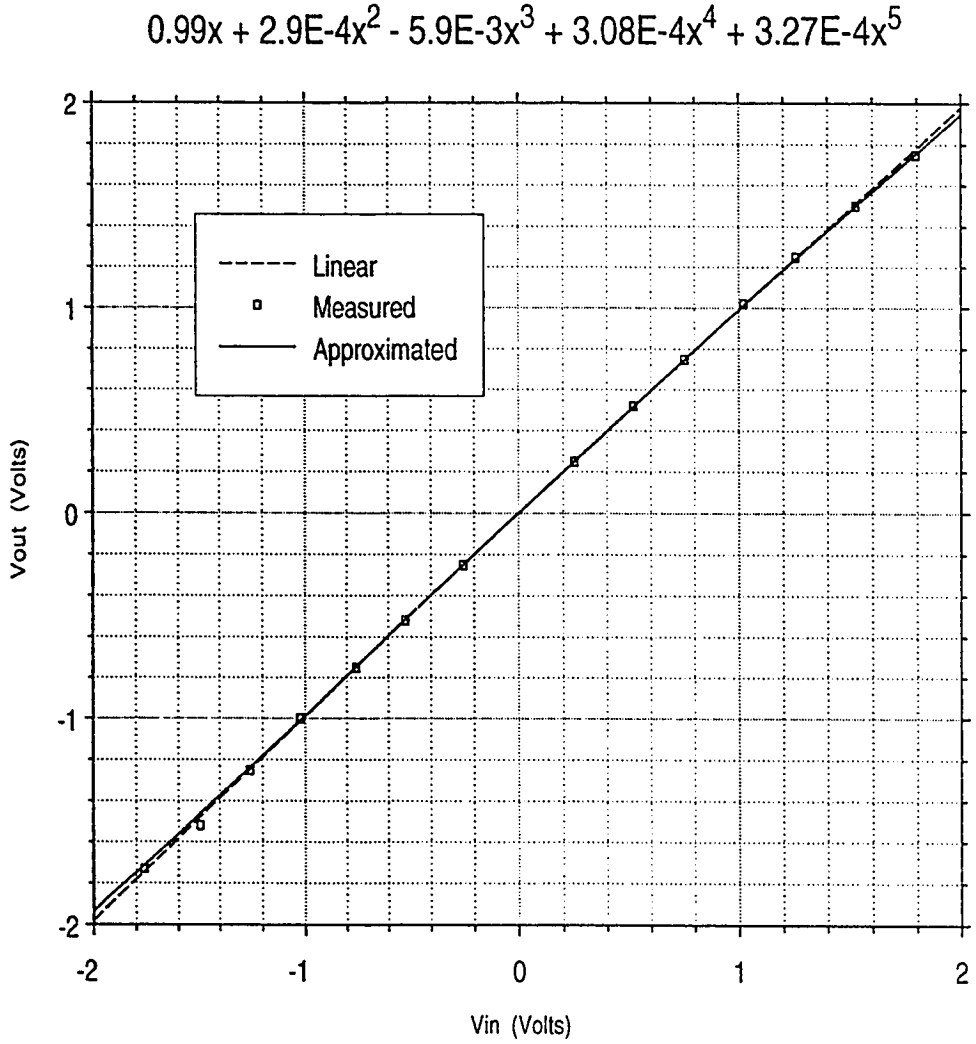

Figure 4.16: Input-Output Characteristics of Band-Reject Filter measured at f_{nom}

	a_n	b_n	c_n	a_d	b_d	c_d
$H(j\omega)$	1	0	1.58E10	1	1.77E4	7.89E9
$G(j\omega)$	1	0	1.55E10	1	1.67E4	8.03E9

Table 4.17: Prefilter and Postfilter Curve-fit Coefficients for Band-Reject Filter

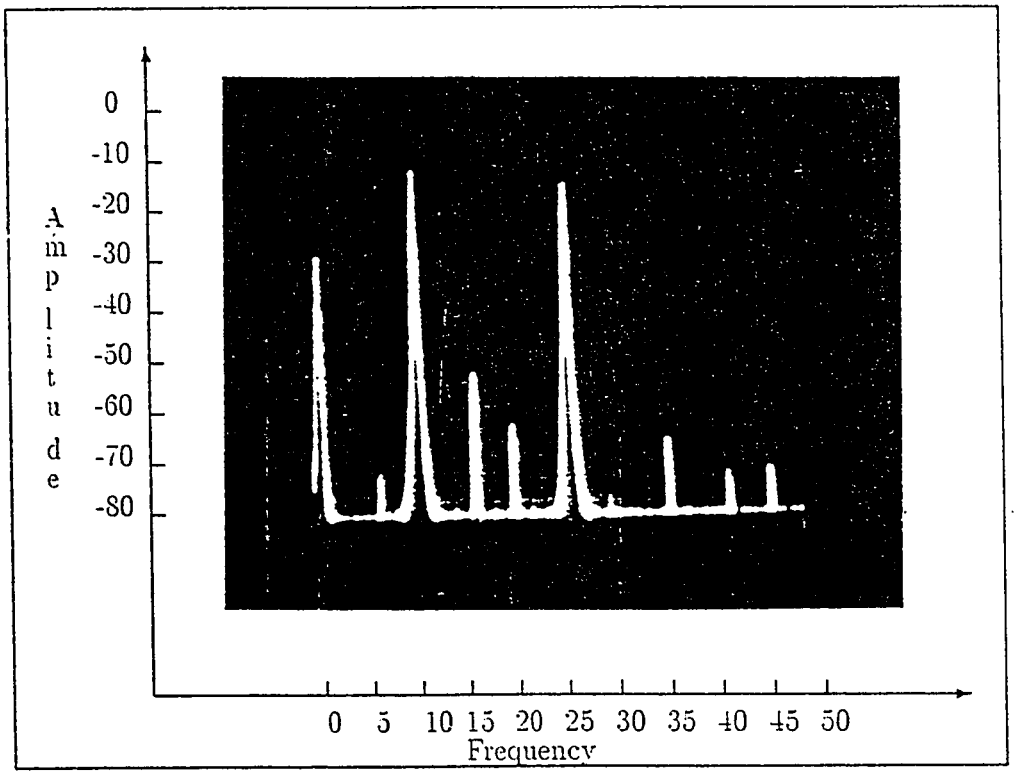

Figure 4.17: Intermodulation Distortion in Band-Reject Filter (f_1=10kHz f_2=26kHz) Amplitude: dBV_{rms}; Frequency: kHz

Harmonics and Intermodulation Products

The measured and predicted amplitudes of harmonics and intermodulation products for band-reject filter are given in Tables 4.18, 4.19, and 4.20. A sample screen image of the spectrum analyzer for measurements is shown in Fig. 4.17.

Harmonic IMP	Freq. (kHz)	V_1= -9dBV V_2= -9dBV			V_1=-15dBV V_2=-15dBV		
		V_M	V_P	E	V_M	V_P	E
$-2f_1+f_2$	6	-69	-66.3	2.7	-	-	-
f_1	10	-9	-9.1	0.1	-15	-15.1	0.1
$2f_1$	20	-63	-63.5	3.5	-80	-82.5	2.5
$-3f_1+2f_2$	22	-78	-75	3.0	-	-	-
f_2	26	-12	-9.7	2.3	-17	-15.6	1.4
$-f_1+f_2$	36	-63	-65.9	2.9	-83	-84.2	1.2

Table 4.18: Amplitudes of Harmonics and Intermodulation Products (dBV_{rms}) for Band-Reject Filter with f_1=10kHz and f_2=26kHz

Harmonic IMP	Freq. (kHz)	V_1= -9dBV V_2= -9dBV			V_1=-15dBV V_2=-15dBV		
		V_M	V_P	E	V_M	V_P	E
f_1	13	-7	-9.3	2.3	-15	-15.2	0.2
f_2	25	-13	-9.9	3.1	-17	-15.8	1.2
$2f_1$	26	-70	-67.9	2.1	-84	-86.8	2.8
$-f_1+2f_2$	37	-60	-58.8	1.2	-75	-75.8	0.8
$3f_1$	39	-68	-68.7	0.7	-	-	-

Table 4.19: Amplitudes of Harmonics and Intermodulation Products (dBV_{rms}) for Band-Reject Filter with f_1=13kHz and f_2=25kHz

Harmonic IMP	Freq. (kHz)	V_1= -9dBV V_2= -15dBV			V_1=-15dBV V_2=-9dBV		
		V_M	V_P	E	V_M	V_P	E
f_1	15	-10	-9.5	0.5	-15	-15.5	0.5
$-f_1+f_2$	16	-82	-85.3	3.3	-80	-85.1	5.1
$2f_1$	30	-70	-74.2	4.2	-	-	-
f_2	31	-14	-15.2	1.2	-11	-9.2	1.8

Table 4.20: Amplitudes of Harmonics and Intermodulation Products (dBV_{rms}) for Band-Reject Filter with f_1=15kHz and f_2=31kHz

4.6 Discussion

The experimetal results of four sample circuits have been presented in the preceeding section to demonstrate the validity of the proposed model. The performance of the model has been tested for various sets of inputs with sinusoids of arbitrary amplitudes and frequencies.

The predicted and measured values of amplitudes of harmonics and intermodulation products were found to be in close agreement. The absolute error between the two is less than 3dB in most cases. From most practical cases, accuracy in prediction of low level unwanted products is seldom required to be better than ±3dB to ±6dB [38, 39, 40, 41].

The existing models of nonlinear systems have not been supplemented by experimental intermodulation analysis. Some efforts have, however, been made to propose such analysis based on mathematical techniques.

Bowron et. al [1] have used the harmonic balance technique to evaluate intermodulation performance in the time domain to study the distortion in various active filter circuits. The error in prediction is reported to be within ±1dB.

The intermodulation-balance technique adopted by Zeng [17], as applied to the prediction of nonlinear distortion effects in filters, results in an error of ±2dB for a two-tone case.

It is, therefore, apparent that the proposed model has an error in prediction

which is within the bounds dictated by most system requirements.

The error in prediction by the proposed model can possibly originate from the cummulative effect of the error introduced by the curve-fitting procedures used at various stages of derivation of the model itself. Visual measurements from the equipment could have resulted in an error of upto $1dBV_{rms}$, especially at low amplitudes.

If the input-output characterictics have terms of higher order than considered, with significant magnitudes, it is possible that the intermodulation prodcuts of higher order overlap and their vector sum contributes to the error.

The amplitudes of carrier signals are predicted with a relatively higher degree of accuracy as compared to the intermodulation products. This behavior can be attributed to the absence of postfilter $G(j\omega)$ in the carrier sinusoid path, hence reduction in the possibility of error due to curve-fitting methods.

Strong nonlinear behavior, as in the case of bandpass filter, resulted in degradation of accuracy. The error, however, remained within the acceptable limits.

Chapter 5

Conclusion and Suggestions for Future Work

5.1 Introduction

A new simplified mathematical model for frequency dependent nonlinear circuits and systems has been proposed in the thesis. In this chapter, some conclusions have been drawn regarding the performance of the proposed model and suggestions have been made for future work in this area.

5.2 Conclusion

The proposed model was evaluated by comparison of computer simulation results and experimental measurements. It was found that the two are in good accordance for most multi-sinusoidal inputs. The amplitude measurements for the carriers, harmonics and intermodulation products at the output validate the model of general mutiple sinusoidal input with arbitrary amplitudes.

The curve-fitting functions used in the derivation are easily implementable on a personal computer and sufficiently accurate seed values for these routines are available from the visual inspection of the plotted data.

An alternate model based on the premise of swept-tone measurements was also presented and was found to be valid only for systems excited by single-tone input sinusoids.

To formulate a complete model for a system, the phase measurements and predictions should also be included. However the hardware required to incorporate the phase measurements is more complex and not readily available.

The accuracy of the predictions by the model is of acceptable degree. The cummulative error introduced by power series truncation, measurement and the curve-fitting procedures was found to remain within prescribed limits [37]. The measured and calculated results have been tabulated along with the absolute error between them.

5.3 Directions for Future Work

The possibility for improvement always exists in research work. Some of the possible directions have, therefore, been stated for researchers desirous of working further in this area. Suggestions have also been included to improve the accuracy of the proposed model.

- The model could be made more effective by including the phase prediction blocks.
- Improvement in the prediction accuracy could be achieved by using the tranfer characteristics between the input and the amplitude of the fundamental frequency at the output
- Accuracy of the predicted results could also be improved by using higher order power series approximation.
- The curve-fitting procedures could be incorporated in the software itself to offer an integrated environment for possible use in real-time applications.
- The performance of model could be evaluated for larger number of input sinusoids with arbitrary amplitudes, including stop-band frequencies.
- An integrated system could be fabricated with data acquisition hardware and supporting software incorporating the proposed model, to implement on-line linearization of nonlinear systems.

Appendix A

A.1 Computation of Intermodulation Products for a Power Series Nonlinearity

Sea [29, 30] has proposed a formula for the computation of amplitudes of harmonics and intermodulation products generated by a nonlinear system described by a power series.

A nonlinear device with input x and output y can be described by the power series

$$y = \sum_{n=0}^{\infty} a_n x^n \tag{A.1}$$

The input is given by the summation of sinusoids $x = x_1 + x_2 + x_3 + \cdots + x_M$ where

$$x_i = E_i \cos\theta_i$$

and $\theta_i = \omega_i t + o_i$. Equation A.1 can therefore be written as:

$$y = \sum_{n=0}^{\infty} a_n \left(\sum_{m=1}^{M} x_m \right)^n \tag{A.2}$$

The output y is composed of the sum of all the distinct terms of the form $V\cos\theta$, where

$$\theta = n_1\theta_1 + n_2\theta_2 + \cdots + n_M\theta_M$$

and the coefficients $n_1, \cdots, n_M$ can take any integer values. V is the amplitude of the harmonic or the intermodulation product. The 'order' of intermodulation product is given by

$$N = |n_1| + |n_2| + \cdots + |n_M| \tag{A.3}$$

The amplitude V can be calculated by the following formula:

$$V = \varepsilon_N \left[\prod_{i=1}^{M} E_i^{|n_i|}\right] \sum_{L=0}^{\infty} \frac{a_{N+2L}(N+2L)!}{2^{N+2L}} \Phi(M, L) \tag{A.4}$$

where

$$\Phi(M, L) = \sum_{q_1} \cdots \sum_{q_M} \prod_{i=1}^{M} \frac{E_i^{2q_i}}{q_i!(|n_i| + q_i)!} \tag{A.5}$$

$\varepsilon_n = 1$ if $N = 0$ and $\varepsilon_n = 2$ if $N = 1, 2, \cdots$.

The computation procedure for implementing the calculation using a computer is described as follows:

If the amplitude V is to be computed by Equation A.4 truncated at $L = L_o$, then it is necessary to compute $\Phi(M, L)$ for $L = 0, 1, \cdots, L_o$. To do this iteratively, $\Phi(1, q)$ for $q = 0, 1, \cdots, L_o$ has to be computed first using

$$\Phi(1, q) = \frac{E_1^{2q}}{q!(|n_1| + q)!}$$

Then for $r = 2, 3, \cdots, M$ compute $\Phi(r, q)$ for $q = 0, 1, \cdots, L_o$ using

$$\Phi(r,q) = \sum_{q_r=0}^{q} \frac{E_r^{2q_r}}{q!(|n_r| + q)!} \Phi(r-1, q-q_r) \tag{A.6}$$

Computing $\Phi(r,q)$ by Equation A.6 is equivalent to evaluating a qth degree polynomial in E_r^2.

The computation software for calculation of amplitudes of harmonic and intermodulation products is listed. The code is written in C language and is valid for band-pass filter response.

```
#include<stdio.h>
#include<conio.h>
#include<math.h>
#include<stdlib.h>

/* Define global variables */
#define M 3     /* No. of input signals+1 */
#define ord 8   /* Max. Order+3 of IMPs & Polynomial Approximation */
#define L0 1    /* N+2*L0 <= ord */
#define pi 3.1415927
FILE *fpin,*fpout;
char namein[20],nameout[20];
float E[M],freq[M],XX[M],a[ord],f;
int i,j,l,n[M],N;

/* Define Functions */
int fact(int x);        /* To calculate factorial */
float calcimp();        /* To calculate IMP magnitudes for the two models */
float postfilter(float Vx); /* Postfilter G(w) T(w) for proposed model*/
/* Universal Filter */
float ufilter(float an, float bn, float cn, float ad, float bd, float cd);

main()
{
float Vact,Vx,Gr,Vprp,VadBV,VpdBV,VxdBV,Err,Fa;
int check;
/* Main body of program START */
input();        /* Input data */
prefilter();    /* Prefilter  */
clrscr();
for(i=-5;i<=5;i++)   /* Generate IMPs */
   {
   for(j=-5;j<=5;j++)
     {
     n[1]=abs(i);
     n[2]=abs(j);
     N=n[1]+n[2];
     f=i*freq[1]+j*freq[2];
     if( f>0 && f<40 && N<=5)
       {
```

```
      printf("\n\n\n (%d) (%d) = %5.2f kHz",i,j,f);
      if( (fpin = fopen(namein,"r")) == NULL)
{
printf("\n Cannot open input file.");
exit(1);
}
      for(l=1;l<M;l++)fscanf(fpin,"%f %f \n",&freq[l],&XX[l]);
      check=1;
      while(check!=0)
   {
   fscanf(fpin,"%f %f \n",&Fa,&Vact);
   if(Fa==f || Fa==0)check=0;
   }
      fclose(fpin);
      /* Proposed model */
Vx=calcimp();
if(Vact!=0 && Vx!=0)
  {
  Vact=2*sqrt(2)*pow(10,Vact/20);      /* dBVrms to p-p conversion */
  printf("\n Vx=%f Vact=%f",Vx,Vact);
  Gr=Vact/Vx;
  printf("\n             Required value of G/T(w)=%f",Gr);
  Vprp=postfilter(Vx);
  if (Vact <0) {Vact=-Vact;}
  if (Vprp <0) {Vprp=-Vprp;}
  if (Vx <0) {Vx=-Vx;}
  VadBV= 20*log10(Vact/(2*sqrt(2)));
  VpdBV= 20*log10(Vprp/(2*sqrt(2)));
  printf("\n Vact=%8.4f Vp-p %8.3f dBVrms",Vact,VadBV);
  printf("\n Vprp=%8.4f Vp-p %8.3f dBVrms",Vprp,VpdBV);
  Err=VadBV-VpdBV;
  printf("\n                      Error= %3.1f dBVrms",Err);
  fprintf(fpout,"%f    %f     %f    %f\n",f,VadBV,VpdBV,Err);
  getch();
  }
      /* End of proposed model */

 /* Main body of program END */
       }
     }
   }
```

```
fclose(fpout);
return;
} /* End of main() */

/* Data Input */
input()
{
float dBV;
clrscr();
printf("\n\n\n\n Enter the input filename[*.IN?]: ");
scanf("%s",namein);
printf("\n\n\n\n Enter the output filename[*.OT?]: ");
scanf("%s",nameout);
if((fpin = fopen(namein,"r")) == NULL)
  {
  printf("\n Cannot open input file.");
  exit(1);
  }
if((fpout = fopen(nameout,"w")) == NULL)
  {
  printf("\n Cannot open output file.");
  exit(1);
  }
clrscr();
for(l=1;l<M;l++)
  {
  fscanf(fpin,"%f %f \n",&freq[l],&E[l]);
  fprintf(fpout,"%f %f \n",freq[l],E[l]);
  E[l]=2*sqrt(2)*pow(10,E[l]/20);    /* dBV to p-p Conversion */
  }
fclose(fpin);
return;
}

/* Prefilter H(w) */
prefilter()
{
float H;
float anH=0,bnH=1.30e6,cnH=0,adH=1,bdH=35.6e3,cdH=1.579e10;
for(l=1;l<M;l++)
  {
```

```
  f=freq[l];
  H = ufilter(anH,bnH,cnH,adH,bdH,cdH);
  E[l]=E[l]*H/(bnH/bdH); /* Normalizing the pass-band gain to unity */
  printf("\n                    E[%d]*H(f%d)=%f",l,l,E[l]);
  }
getch();
return;
}

/* Calc. IMPs for proposed model */
float calcimp()
{
int q,r,qr,L;
float phi[5][4],den,num,sum,prod,k,V,en=2;
     a[1]=45.1;
     a[2]=2.38;
     a[3]=-29.4;
     a[4]=13.0;
     a[5]=-35.93;
     a[6]=0;
     a[7]=0;
for(r=1;r<M;r++) {for(q=0;q<=L0;q++) {phi[r][q]=0;}} /* Initialze */
for(q=0;q<=L0;q++)
  {
  phi[1][q]=(pow(E[1],2.00*q))/(fact(q)*fact(n[1]+q));
  }
for(r=2;r<M;r++)
  {
  for(q=0;q<=L0;q++)
    {
    for(qr=0;qr<=q;qr++)
      {
      den=fact(qr)*fact(n[r]+qr);
      num=pow(E[r],2.00*qr);
      phi[r][q]=phi[r][q]+ phi[r-1][q-qr] * (num/den);
      }
    }
  }
prod=1;
for(l=1;l<M;l++)
  {
```

```
  prod=prod*pow(E[l],n[l]);
  }
sum=0;
for(L=0;L<=L0;L++)
  {
  k=N+2*L;
  sum=sum + phi[M-1][L]*((a[k]*fact(k))/(pow(2,k)));
  }
V=en*prod*sum;
return(V);
}

/* Postfilter G(w) & T(w) for proposed model */
float postfilter(float Vx)
{
float Vp,G,w;
float anG=0,bnG=46.27e3,cnG=0,adG=1,bdG=35.6e3,cdG=1.579e10;
if(N==1)
  {
  /* Carrier Post Filter T(w) */
  Vp=Vx;
  printf("                    Carrier!");
  }
else
  {
  /* IMP Post Filter G(w) */
  G=ufilter(anG,bnG,cnG,adG,bdG,cdG);
  printf("\n Calculated value of G(w)=%f",G);
  Vp=Vx*G;
  printf("                    IMP!");
  }
return(Vp);
}

/* Universal Filter Function */
float ufilter(float an, float bn, float cn, float ad, float bd, float cd)
{
float X,w;
w=2*pi*f*1e3;
X=(sqrt( (pow(cn-an*pow(w,2),2)) + (pow(bn*w,2)) )) / (sqrt( (pow(cd-ad
*pow(w,2),2)) + (pow(bd*w,2)) ));
```

```
return(X);
}

/* Factorial function */
int fact(int x)
{
int j,y=1;
if(x==0 || x==1) {y=1; goto last;}
for(j=x;j>=2;j--) {y=y*j;}
last: return(y);
}
```

A.2 Selection of Input Frequencies for Distinct Harmonics and Intermodulation Products

As pointed out earlier, it is essential that the input frequencies are selected such that the harmonics and intermodulations products generated by a system, which is approximated by a finite order power series, do not overlap. This feature is included to enhance the accuracy or results and eliminate the possibility of error arising from spurious frequency component sharing the same spectral zone with those under consideration.

Since phase effects have not been taken into account while modeling the system, it is mandatory that frequency overlapping be avoided by suitably locating the input frequencies and avoid vectoral addition of frequency components at the output.

A program listing is giving to generate such a set of frequencies. The code is written in C language and is valid for fifth order power series nonlinearity excited by two sinusoids lying in the pass-band of the band-reject filter.

```
#include<stdio.h>

main()
{
int r,f1,f2,f3,n1,n2,n3,an1,an2,an3,f,i,j,k,N;
int wa1=10,wa2=25,wb1=10,wb2=25;
int ord=5,dum[100];

clrscr();
for(f1=wa1;f1<=wa2;f1++)
  {
  for(f2=wb1;f2<=wb2;f2++)
    {
      printf("\n\n\n ***%d %d***       ",f1,f2);
      j=0;
      r=0;
      for(i=0;i<100;i++) {dum[i]=0;}
if(f1!=f2)
{
for(n1=-ord;n1<=ord;n1++)
  {
  for(n2=-ord;n2<=ord;n2++)
    {
      f=(n1*f1)+(n2*f2);
      an1=abs(n1);
      an2=abs(n2);
      N=an1+an2;
      if(f>0 && f<40 && N<=ord)
{
printf("\n N=%d (%d) (%d)    f=%d       ",N,n1,n2,f);
for(k=0;k<100;k++) {if(dum[k]==f) {r=r+1;}}
dum[j]=f;
j=j+1;
}
      }
  }
  printf("No. of Repeated Freq.=: %d",r);
  getch();
      }
    }
```

```
  }
return;
}
```

Bibliography

[1] P. Bowron and A.A. Muhieddine. "Large-Signal Multitone Excitation in Analogue Active Filters". *IEE Colloq. on Digital and Analogue Filter and Filtering Systems*, 187(10):1–4, 13 December 1991.

[2] P. Bowron and A.A. Muhieddine. "Active Filters with Reduced Harmonic Distortion". *IEE Colloq. on Digital and Analogue Filter and Filtering Systems*, 91(9):1–5, 25 May 1990.

[3] R.S. Moni and K.R. Rao. "Jump Phenomenon in Active-RC Filters". *IEEE Transactions on Circuits and Systems*, CAS-29(1):54–55, 1982.

[4] R. Blum and M.C. Jeruchim. "Modeling of Non-linear Amplifiers for Communication Simulation". *International Conference on Communication*, 48(3):1–5, 1989. 1989.

[5] V. Volterra. *Theory of Functionals and Integro-Differential Equations*. Dover, New York, 1959.

[6] A.C. Heathman and J.G Gardiner. "Accuracy Considerations in Approximate Representation of Non-linear Two-ports". *European Conference on Circuit Theory and Design*, B1(4):178–181, 1985.

[7] P. Hetrakul and D.P. Taylor. "Nonlinear Quadrature Model for a Travelling-Wave-Tube Type Amplifier". *Electronics Letters*, 11(2):50, 23 January 1978.

[8] O. Shimbo. "Effects of Intermodulation, AM-PM Conversion and Additive Noise in Multicarrier TWT Systems". *IEEE Proceedings*, 59(2):230–238, February 1971.

[9] M.J. Eric. "Intermodulation Analysis of Nonlinear Devices for Multiple Carrier Inputs". *Communication Research Centre Report*, 1234, November 1972. CRC, Ottawa, Ontario, Canada.

[10] A.A.M. Saleh. "Frequency-Independent and Frequency-Dependent Nonlinear Models of TWT Amplifiers". *IEEE Transactions on Communications*, 29(11):1715–1720, November 1981.

[11] H.B. Poza, Z.A. Sarkozy, and H.L. Berger. "A Wideband Datalink Computer Simulation Model". *Proceedings of NAECON*, pages 71–78, 1975. National Aeronautical Engineers Conference Record '75.

[12] M.T. Abuelma'tti. "Frequency Dependent Nonlinear Quadrature Model for TWT Amplifiers". *IEEE Transactions on Communications*, 32(8):982–986. August 1984.

[13] T. Sasaki and H. Hataoka. "An Intermodulation Prediction and Measurement Technique for Multiple Carriers through Weak Nonlinearities". *IEEE Transactions on Cable Television*, 4(4):146–154, October 1979.

[14] P. Bowron and M.A. Mohamed. "Amplifier Nonlinearities in the Multiple-Negative-Feedback Bandpass Filter". *International Journal of Circuit Theory and Applications*, 6:121–134, 1978.

[15] P. Bowron and A.P. O'Carroll. "Harmonic-Balance Evaluation of Large-Signal Behaviour of Active Filters". *IEE Colloq. on Modelling and Analysis of Circuits and Devices*, 111(15):1–5, 4 December 1987.

[16] M.T. Abuelma'atti. "Prediction of RFI demodulation in bipolar operational amplifiers". *IEE Proceddings*, 135 Pt.G(1):29–33, February 1988.

[17] X. Zeng, P. Bowron, and A.A. Muhieddine. "Nonlinear distortion prediction of active filters". *Electronics Letter*, 30(7):553, 31 March 1994.

[18] A. Nasser, M. Fikri, and K. Kafrawy. "Volterra Series Analysis of Intermodulation Distortion in Second-Order Filters.". *IEEE Circuits and Systems Magazine*, pages 4–8, June 1983.

[19] A.S.S. Al-Kabbani and P. Bowron. "Behaviour of Actively Compensated Band-pass Filters at Higher Signal Levels". *Electronics Letters*, 23(21):1108–1109, 8 October 1987.

[20] B. Arnold. "Third Order Intermodulation Products in a CATV Systems". *IEEE Transactions on Cable Television*, CATV-2(2):67–76, April 1977.

[21] A. Borys. "On Intermodulation and Harmonic Distortion in Single-Amplifer Active Filters". *Journal of Audio Engineering Society*, 28:706–712, October 1980. Correction 29:443, June 1981.

[22] P.J. Billam. "Harmonic Distortion in a class of Linear Active Filter Networks". *Journal of Audio Engineering Society*, 26:426–429, June 1978.

[23] L. Kristian and A. Forsen. "Analysis of Nonlinear Model for Operational Amplifers in Actice RC Circuits". *Circuit Theory and Applcations*, 2:13–22, 1974.

[24] A.L. Berman and C.H. Mahle. "Nonlinear phase shift in traveling-wave tubes as applied to multiple access communication satellites". *IEEE Transactions on Communication Technology*, COM-18:37–48, February 1970.

[25] C.M. Thomas, M.Y. Weidner, and S.H. Durrani. "Digital amplitude-phase keying with M-ary alphabets". *IEEE Transactions on Communications*, COM-22:168–180, February 1974.

[26] M. T. Abuelma'atti and J. G. Gardiner. "Input power assignment of equal-amplitude multicarrier systems for given carrier power". *International Journal of Electronics*, 50:55–60, 1981.

[27] O.J. Bonello. "Distortion in Postive and Negative-Feedabck Filters". *Journal of Audio Engineering Society*, 32(4):239–244, April 1984.

[28] M.T. Abuelma'atti. "A simple algorithm for fitting measured data to Fourier series models". *International Journal of Mathematics Education Science and Technology*, 24(1):107–112, 1993.

[29] R.G. Sea. "An algebraic formula for amplitudes of intermodulation products involving an arbitrary number of frequencies". *IEEE Proceedings*, 56:1388–1389, August 1968.

[30] R.G. Sea. "On the Computation of Intermodulation Products for a Power Series Nonlinearity". *IEEE Proceedings*, 57:337–338, March 1969.

[31] Wai-Kai Chen. *Passive and Active Filters: Theory and Implementations*. John Wiley and Sons, 1986.

[32] M.S. Ghausi and K.R. Laker. *Modern Filter Design: Active RC and Switched Capacitor*. Prentice Hall Inc., 1981.

[33] H. Y-F. Lam. *Analog and Digital Filters: Design and Realization*. Prentice Hall Inc., 1979.

[34] W.C. Nuyen and P.P.L. Regtien. "The Influence of Non-linearity in Active Filters". *International Journal of Electronics*, 41(3):241-247, 1976.

[35] A.S. Sedra and P.O. Brackett. *Filter Theory and Design: Active and Passive.* Matrix Publishers Inc., 1978.

[36] S.A. Maas. *Nonlinear Microwave Circuits.* Artech, 1988.

[37] M.T. Abuelma'atti. "Reduction of Intermodulation in Communications Amplifiers by Pre-Correction Techniques". *Ph.D. Dissertation*, 1979. University of Bradford.

[38] J.G. Gardiner. "Computer Modelling of Non-linear Interactions between Co-sited Transmitters". *Proceedings of IERE Conference on Civil-land Mobile Radio*, 33:123-132, 18-20 November 1975.

[39] L.M. Orloff. "Intermodulation Analysis of Crystal Mixer". *IEEE Proceedings*, 52:173-179, February 1964.

[40] N.A.A. Makia. "Spectrum Evaluation for Multi-Carrier Transmission through Systems with Saturating Characteristics". *Ph.D. Dissertation*, 1973. University of Bradford.

[41] J.G. Gardiner. "Evaluation of Intermodulation Spectra in Mixers, Modulators and Related Devices Operating between Resonant Terminations". pages 424-

432, September 1972. NATO Advanced Study Institute on Network and Signal Theory, Bournemouth, Hants, England.

Vita

- Fahim Shafi
- Born in Lahore, Pakistan.
- Received Bachelor of Science degree in Electrical Engineering from the University of Engineering and Technology, Lahore, Pakistan in September, 1992.
- Completed Master of Science degree requirements at King Fahd University of Petroleum and Minerals, Dhahran, Saudi Arabia in December, 1994.